Response to Editor's and Reviewers' Comments on Manuscript hess-2020-91 "A new criterion for determining the representative elementary volume of translucent porous media and inner contaminant" by Ming Wu, Jianfeng Wu, Jichun Wu, and Bill X. Hu

Note that the following text in Arial Narrow font denotes Editor's and Reviewers' comments and in Times New Roman font denotes our response to the comments in the review. In our Supplement (pdf/zip), the PDF file has clearly indicated all changes to the original manuscript. In our Manuscript (pdf), all changes have been included in the clean version of the revised PDF file. Also, in our marked PDF file, marked in ~~a green strikethrough font~~ is the text that should be removed from the original manuscript and marked in red font is the text that has been added to the revision. In addition, Line number(s) mentioned below is referred to as that line numbering in the marked revised manuscript.

Response to Anonymous Referee #1's Comments

Anonymous Referee #1

Received and published: 24 June 2020

This paper presents a study of determining the REV of translucent porous media and inner contaminant based on two sand-box experiments. This paper is interesting, however, some details are missing. So I suggest "Major revision".

[Response] Comments accepted. We appreciate Referee #1's conscientious and positive recommendation. We have fully addressed Referee #1's concerns in the revised manuscript.

My comments are as follows.

(1) In the abstract, the new method of determining criterion should be pointed out clearly.

[Response] Comments accepted. We have revised this sentence to point out the new criteria (Lines 14-16).

(2) Light transmission techniques are very useful in two experiments. As shown in Eqs. (1)-(5), some parameters are important, but these parameters are not introduced in the following experiments and analysis.

[Response] Comments accepted. We have added a heterogeneous case (Experiment-III) to validate the applicability of new criteria for REV estimation.

To derive two fitting constants, some procedures should be taken. For heterogeneous case

(Experiment-III), six grades of commercial translucent Accusand silica sand were used to pack the sandbox. Background material was packed by the F20/30 mesh sand and F70/F100, F70/F80, F40/F60, F50/F70, F35/F50 mesh sands with low permeability were used to pack five lenses (Fig. 2c and Table A1).

Table A1 Properties of six kinds of translucent silica sand

Property of sands	F20/30 background	F30/40 Lens E	F50/70 Lens D	F40/50 Lens B	F70/80 Lens C	F70/100 Lens A
Median grain diameter (cm) [a]	0.072	0.036	0.026	0.034	0.022	0.016
Porosity [b]	0.331	0.304	0.249	0.277	0.221	0.201
Permeability (m^2) [a]	1.35×10^{-10}	8.85×10^{-11}	3.66×10^{-11}	6.38×10^{-11}	8.19×10^{-12}	4.69×10^{-12}
Entry pressure (kPa) [a]	0.049	0.203	1.058	0.490	2.048	3.895

[a] refer to O'Carroll et al. (2004)

[b] from experiment measurement and refer to Bradford et al. (1999)

Temporal emergent light intensity distribution before PCE injection into sandbox was collected as in Fig. 3a which every pixel is 0.482mm×0.523mm. Obviously, area of every pixel approaches zero and obey the requirement of Light transmission technique. The average emergent light intensity of lenses A, B, C, D, E and background material F20/30 mesh sand are derived from Fig. 3a and their porosity is listed in Table A1. The relationship between light intensity and porosity developed by Light transmission technique as Eqs. (1)-(5) is validated in Fig. A1. There is a fairly agreement between light intensity and porosity with R^2 value equals to 0.9818 that any significant bias doesn't appear in the validation results (Fig. A1). The parameters γ and β in Eq. (5) are achieved from validation results and the porosity distribution of 2D porous media achieved by Light transmission technique is shown in Fig. A1. The whole mass of sand packed in the sandbox is calculated:

$$M_c = \sum_{i_2}^{m_2}\sum_{i_1}^{m_1}(1-\theta_{i_1,i_2})L_1L_2L_3\rho_s \tag{A1}$$

where M_c is the total mass of sand calculated from Light transmission technique; i_1 is the layer number of computing grid; i_2 is the row number of computing grid; m_1 is total number of layers; m_2 is the total number of rows; $\theta_{i,j}$ is the porosity of computing grid; L_1 is the length of computing grid; L_2 is the width of computing grid; L_3 is the thickness of computing grid; ρ_s is the density of sand particles. In comparison with the actual mass of sand in experiment, the relative error of 4.85% is achieved by Light transmission technique for calculation of sand mass. These results indicate a good agreement between the quantifications by Light transmission technique and experiment observations.

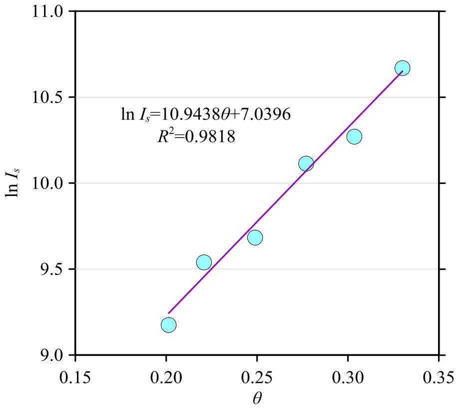

Fig. A1 The emergent light intensity versus porosity for different mesh sands used in experiment.

For other experiments, the emergent light intensity is corrected using the method expressed by Bob et al. (2008). All images collected were automatically corrected for the dark signal (baseline) associated with the CCD detector by subtracting an image taken at the same exposure time with the camera shutter closed. To correct for the inevitable temporal variation in light intensity, a small region, referred to as a "correction box", in one of the collected images (referred to as the reference image) was identified. The reference image was chosen to be the image collected when the model was fully saturated with water and was packed by background material (F20/30 mesh sand) for Experiment-III. In choosing the correction box, it was very important to make sure that, for all other images of Experiments-I and II, this region always remained under the same conditions of full water saturation and same mesh sand. Thus, any change in light intensity within the correction box was due to changes in source light intensity. The average light intensity of this correction box was calculated for all images including the reference image. To correct a particular image of other experiments, light intensities from image were simply multiplied by the ratio of the average light intensity of the correction box for the reference image and the average light intensity of the correction box for the image to be corrected.

Afterward, porosity is quantified by Eq. (5). Then density and tortuosity can be achieved using Eqs. (6) and (7).

(3) In Lines 141-142, an assumption that the particles and pores are with lamellar structure is made. Further explanation and justification should be made for the reasonability of the assumption.

[Response] Comments accepted. To quantify the porosity of translucent silica sand by light transmission method, we suppose 2D translucent silica sand is consist of various infinitesimal elements whose area approaches zero. An infinitesimal element is selected from 2D translucent silica sand which area approaches zero (Fig. 1d). The size of cross-sectional area of infinitesimal element is less than the particle size of silica sand. Therefore, the infinitesimal element can be treated as lamellar structure shown in Fig. 1d. Obviously, area of every pixel approaches zero and obey the requirement of Light transmission technique. In comparison with the actual mass of sand in experiment, the relative error of 4.85% is achieved by Light transmission technique for calculation of sand mass.

(4) From Figure 7, the pattern of minimum REV sizes of porosity, sand density and torturosity is quite different. Further explanation should be given based the new criterion.

[Response] Comments accepted. The materials packed in two sandboxes are different. F40/50 and F20/30 mesh translucent silica sands are used for Experiments-I and II. So the minimum REV sizes of two experiments are different. What's more, the REV sizes of different parameters have different patterns. The REVs of porosity, moisture saturation (S_W) and interfacial area (A_I) also obtained different values according to Costanza-Robinson et al. (2011). The relationship observed for S_W-REV and S_W are different from the relationship between A_I-REV and S_W. Therefore, the REV of different parameter is possible to be different.

(5) The innovative point of this paper lies in the proposed criterion of determining REV. Two experiments have been carried out to validate the accuracy and reasonability of the criteria. However, the applicability of this method still requires to be further validated and clarified, because two cases are not enough and scale effects exists.

[Response] Comments accepted. We have added a heterogeneous case (Experiment-III) into the revised manuscript (Fig. 2c).

(6) The mean size of REV is made based on its relations with porosity, density and tortuosity. Other variables, such as pressure or saturation, can be served as an additional indicator?

[Response] Comments accepted. The REV of porous media is made based on its relations with porosity, density and tortuosity. However, PCE saturation is an indicator for PCE plume in porous media, the REV of PCE saturation can be used to obtain the REV of PCE plume.

Minor comments:

(1) In Line 14, what are "previous REV estimation"?

[Response] Comments accepted. We have corrected "previous REV estimation criteria" to "existing REV estimation criteria" (Lines 14-15).

(2) In Line 15, a new criterion should be clarified.

[Response] Comments accepted. We have made correction to clarify the new criterion (Lines 14-17).

(3) In Line 23, cannot ?

[Response] Comments accepted. We have replaced 'can not' with 'are not effective' (Line 25).

(4) In Line 51-52, Fig.1c is cited before Fig.1a and 1b.

[Response] Comments accepted. We have modified the numbers of figures in Fig. 1 (Lines 653-659, 683-685).

(5) In Line 119, Table1 should be "Table 1".

[Response] Comments accepted. We have corrected "Table1" to "Table 1" (Line 128).

(6) In Lines 217-218, the sub and sup i should be consistent.

[Response] Comments accepted. We have corrected the sub and sup i (Line 256).

(7) In Line 552, volume?

[Response] Comments accepted and correction made accordingly (Line 618).

(8) In Table 1, how do you know permeability of the sand?

[Response] Comments accepted. The average permeability of silica sand is obtained by experiment and research references. Moreover, accurate permeability of 2D translucent silica sand can be calculated by the help of light transmission technique and fractal method. Afterward, average permeability of silica sand also can be obtained.

(9) In Line 623, the subtitle of Fig.5a can be confusing, and it is suggested to replace porosity, density and tortuosity with other words.

[Response] Comments accepted. We have made correction according to suggestion (Lines 703-705).

Response to Anonymous Referee #2's Comments:

Anonymous Referee #2

Received and published: 2 July 2020

This paper proposes a new criterion for identifying representative elementary volume (REV) of translucent silica sands. Two sandbox experiments were conducted to test the applicability of the proposed criterion. The authors stated that the proposed criterion is effective and reliable. However, there are some important issues in the current manuscript that should be resolved or addressed.

[Response] Comments accepted. We appreciate Referee #2's positive comments. We have fully addressed the concerns raised by Referee #2's in the revised manuscript to improve the manuscript and given a point-to-point response to the reviewer's comments as below.

Major comments:

1. The authors have published a series of paper on this topic. The research gap and the reason why a new criterion for REV is need should be clearly stated in the Introduction section.

[Response] Comments accepted. We have added associated description into the Introduction section (Lines 90-93).

2. Is the proposed criterion purely empirical or with some physical basis? If it is a criterion with physical basis, then the physical basis or the derivation process should also be added.

[Response] Comments accepted. The new criterion conforms to the Eq. (12). Moreover, the new criterion is proposed based on the dimensionless range (δ^i) (Brown and Hsieh, 2000). However, $\delta^i << 1$ is hard to be achieved. According to the $\frac{\partial Y(L_i)}{\partial L}|_{L_i=L_o}=0$ [Eq. (12)], we propose a new criterion $\chi^i=\frac{|\delta^{i+1}-\delta^{i-1}|}{\delta^i \Delta L}$ and test the effect for translucent porous media.

3. The blue curve of II-1 in the last figure of Fig. 4 is totally different from other curves. For other curves, the blue line becomes zero when the read line is zero. But for this figure, the blue line has a very big peak when the red line becomes zero. So the results of this figure are totally different from other figures. Such results seem does not support the authors' conclusion that "...is more convenient and reliable than other methods for REV estimation" in Lines 315-316.

[Response] Comments accepted. Referee #2 may refer to the S_o-χ^i of II-1. The blue line becomes zero when L<5.0mm, suggest the REV size of S_o for II-1 has small value compared to II-2. In the last figure of Fig. 4, the blue line first becomes zero when red line has large value. As scale increases, the red line becomes zero while the blue line has large value again. The phenomenon suggests the S_o-REVs of II-1 and II-2 have different values. By the help of the new criterion, REV estimation is more convenient. To make zero part of blue line more apparent, the blue line is thickened in the last figure of Fig. 4. We have used open circles to indicate the REV plateau region in Fig. 4. Readers can see REV plateau estimated by the new criterion. (Lines 697-700)

4. The authors stated that "All observation cells show similar variation curves of ... that low value intervals are quite apparent, indicating that ... is vary effective to make the REV plateau obvious...", but it is not the case for the last figure in Figure 4b. As very different curves are obtained for Experiments I and II, it should be doubted that whether the new criterion is effective or not. Although the REV plateau may be identified based on the other figures in this study, but it is possibly that the REV plateau cannot easily be identified in other similar studies or in real porous materials.

[Response] Comments accepted. Curves all have low value intervals in Fig. 4 for S_o-χ^i, so we treat these curves as similar variation curves. In the last figure in Fig. 4b, the low value interval of blue line is not apparent, so the blue line is thickened to make the low value interval apparent. (Lines 697-700)

5. The fit to cumulative frequency in Figure 5b is not very good. Both underestimation and overestimation exist.

[Response] Comments accepted. We have made effect to improve the fit to cumulative frequency in Fig. 5b (Lines 703-705).

6. Can the proposed criterion be applied to real world porous materials? Is the proposed criterion only applicable to the translucent silica sand used in this manuscript?

The authors stated that fluid migration and transformation in porous media can be accurately simulated using the light transmission technique and the proposed criterion.

Should the proposed criterion be used with the light transmission technique simultaneously?

If yes, then the applicability of the proposed criterion is restricted to a very narrow range.

[Response] Comments accepted. We appreciate the reviewer's insightful comment. In this study, we only focus on characterizing the REV of translucent silica sand and inner PCE plume at lab scale based on light transmission technique. Due to multiple limitations of x-ray and gramma ray causing high cost, inefficiency, complex high energy sources and hazard environment in materials measurements, light transmission technique is used to achieve rapid, hand and economical measurements of materials with high resolution and good effectiveness. However, minimum REV size (L_{min}) and maximum REV size (L_{max}) can't be identified simultaneously for translucent silica sand based on previous criteria and light transmission technique. So this new criterion is proposed to improve the effect of REV estimation for translucent silica sand. In this study, the proposed criterion is used with the light transmission technique. However, we believe its potential applicability can't be treated as a narrow range by this study. We think this issue is beyond this study and the applicability of the new criterion will be explored in our further work.

Minor comments:

1. Line 51: The authors used n to represent porosity, but then they used to represent porosity in Line 145. The authors again used n to represent porosity in Line 148 Equation (5).

[Response] Comments accepted. We have replaced 'n' with 'θ' (Lines 53 and 158).

2. Line 127: What are the variation ranges of i and j in Equation (1)? They should be added to the equation.

[Response] Comments accepted. We have used *a* and *b* in Eq.(1) to represent phase number and interface number (Lines 136-138).

3. Line 134: Add references to Equation (2)

[Response] Comments accepted. We have added references to Equation (2) (Lines 143-144).

4. Line 142: Add references to Equations (3) and (4)

[Response] Comments accepted. We have added reference to Equations (3) and (4) (Line 152).

5. Line 149: The quantity Ls seems not defined

[Response] Comments accepted. We have checked carefully and made correction (Line 159).

6. Line 169: Is the "Hsies" should be "Hsieh"?

[Response] Comments accepted and correction made (Line 205).

7. Lines 175-176: Reputation: "the derivative... will tend to zero"

[Response] Comments accepted. We have deleted "the derivative... will tend to zero" (Lines 211-212).

8. Lines 176-177: References should be added to this sentence.

[Response] Comments accepted. We have added references (Line 214-215).

9. Line 182: Cannot find i in Figure 1b

[Response] Comments accepted. The cuboid window is presented in Fig. 1b, i refers to the window increment number. We have modified the numbers of figures in Fig. 1 (Lines 653-659, 683-685).

10. Line 194: Here is , in Equation (11) is , which one is correct?

[Response] Comments accepted. The cuboid window is presented in Fig. 1b, i refers to the window increment number. m(i) is the total number of sub-grids in measured cuboid window.

11. Lines 217-218: The authors should carefully check whether i should be in subscript or superscript.

[Response] Comments accepted. We have corrected the sub i to sup i (Line 256).

12. Lines 218-220: Double check whether or should be used.

[Response] Comments accepted. We have checked carefully and corrected the subscripts and superscripts (Line 256).

13. Line 238: Cannot find t=1.44 min in Figure 3b.

[Response] Comments accepted. We have corrected this mistake (Line 278).

14. Lines 239-240: There should be error in this sentence or grammatical error

[Response] Comments accepted. We have revised this sentence (Lines 278-280).

15. Line 243: There is no Fig. 2c

[Response] Comments accepted. We have deleted "Fig. 2c" (Line 180).

16. Line 253: Should be "Figs. 4a and b"

[Response] Comments accepted. We have made correction (Line 293).

17. Line 269: There is no Fig. 4f, only Fig. 4a and 4b in this figure.

[Response] Comments accepted. We have replaced "Figs. 4a-f" to "Figs. 4a and b" (Line 310).

18. Line 338: Use a different symbol in Equation (16), because has already been used in Equation (15).

[Response] Comments accepted. We have used a different symbol (Lines 377-378).

19. Line 358 and 359: Both are Experiment II?

[Response] Comments accepted. All mean REV sizes of these variables for Experiment-II are larger than REVs of Experiments-I. We have made corresponding correction (Line 402).

20. Line 618: The subscripts and superscripts in the axis titles of Figure 4 can not be clearly seen

[Response] Comments accepted. We have revised Figure 4 to make subscripts and superscripts clearer (Lines 697-700).

21. The equations listed in Table 2 are already included in the main text as Equations (10), (11), (14), and (15). Table 2 should be deleted. Also delete the citations and descriptions on Table 2.

[Response] Comments accepted. We have deleted Table and associated citations and descriptions (Lines 627-628).

22. I would suggest the authors modifying the numbers of figures and make sure the figure numbers appear in order in the text. For example, the authors first cited Fig. 1c in Line 52 and then Fig. 1a in Line 96 and Fig. 1b in Line 140. Generally, we should fist cite Fig. 1a, then Fig. 1b, and then Fig. 1c in order.

[Response] Comments accepted. We have modified the numbers of figures in Fig. 1 (Lines 653-659, 683-685).

23. Table 3: Delete the equations and just list the parameter values.

[Response] Comments accepted. We have deleted the equations and list parameter values in Table 2 (Lines 630-634).

Response to Anonymous Referee #3's Comments:

Review on "A new criterion for determining the representative elementary volume of translucent porous media and inner contaminant"

Wu et al. proposed a new criterion to determine the representative elementary volume (REV) of translucent porous media and inner contaminant, compared the new criterion with previous methods in two sandbox experiments, used the new criterion to calculate REVs of PCE plume (such as saturation, PCE-water interfacial area), and analyzed the influence of saturation on the REVs of saturation and PCE-water interfacial area. Although I do see some improvements of the new criterion in the Figure 4, the current paper is not suitable for the publication in HESS journal and needs major revision.

[Response] We appreciate Referee #3's positive comments. Also, we have fully addressed the issues raised by the reviewer and made major revision in the revised manuscript, and given a point-to-point response to the reviewer's comments as follows.

Detailed comments are as follows.

Major comments:

(1) The title of the paper emphasizes on the new criterion, but only Figure 4 shows the comparison between the new criterion and other methods. Why do you design the new criterion as the current form? Why the new criterion has such improvements compared with other methods? These need to be introduced and discussed.

[Response] Comments accepted. We have added more expression into the Introduction section. The new criterion conforms to the Eq. (12). Moreover, the new criterion is proposed based on the dimensionless range (δ^i) (Brown and Hsieh, 2000). However, $\delta^i << 1$ is hard to be achieved. According to the $\frac{\partial Y(L_i)}{\partial L}|_{L_i=L_o}=0$ [Eq. (12)], we propose a new criterion $\chi^i = \frac{|\delta^{i+1}-\delta^{i-1}|}{\delta^i \Delta L}$ and test the effect for translucent porous media. The results suggest the new criterion appears to be the most appropriate criterion for REV plateau identification (Lines 90-93, 253).

(2) Half part of the paper focuses on the "REVs of material properties" and "REVs of So and AOW for PCE plume", but there is no introduction on those topics in the "introduction" section. This makes it confusing on the contribution of this paper as compared with previous research.

[Response] Comments accepted. We have added REVs of material properties and PCE saturation, PCE-water interfacial area in the introduction section (Lines 71-72, 84-88).

(3) The experimental design is not introduced clearly. For example, why do you use two sandboxes with

different materials? Why do the two sandboxes have different size? How to observe different variables with different cuboid window scale? Moreover, I think the method and result are mixed in the current paper. For example, L241-251 and L364-373 are methods instead of the results, so the author should move them to the section 2 to clarify the whole procedure you performed.

[Response] Comments accepted. We have added a heterogeneous case (Experiment-III) to validate the applicability of new criteria for REV estimation. The methods are moved to the section 2 (Lines 176-201).

(4) The figure organization makes the paper not easy to follow. Figures are introduced from Fig. 1c to Fig. 1a, then to Figs. 2a-b, then back to Fig. 1b. I suggest the author to reorganize the figures just as the orders they appear in the paper.

[Response] Comments accepted. We have modified the numbers of figures in Fig. 1 (Lines 653-659, 683-685).

(5) Figure 4. I see the difference of REV determined by "the relative gradient error" and "the new criterion method", which one we should trust? How to approve that the REV calculated by new criterion method is more reliable? Moreover, you can highlight the REV region in Figure 4 so that readers can directly see that.

[Response] Comments accepted. The relative gradient error is proposed by previous study and has also used for our research about translucent porous media and contaminants migration. However, random fluctuations exist in ε_g^i curves visually, which make the REV plateau uneasy to be identified. Significantly, the curve of new criterion appears low value interval which makes the beginning and ending of REV plateau easier to be identified. We have used open circles to indicate the REV plateau region in Fig. 4. Readers can see REV plateau estimated by the new criterion.

(6) Figure 6. There is not any interpret or discussion on the Figure 6. If the figure is important, please provide detail description. If not, I suggest moving it to the supplementary.

[Response] Comments accepted. Fig.7 is obtained on the REV distribution presented in Fig. 6. We have added more discussion about Fig.6 in revised manuscript (Lines 407-419).

(7) L383-384. In the downright corner of the Figure 7a, the red line increases first, then decrease. So I do not agree with that "while REV of PCE plume presents apparent decreasing ... for Experiment-II".

[Response] Comments accepted. We have revised this sentence in revised manuscript (Lines 447-448).

Minor comments:

(1) L54, "As measured scale size ranging between Lmin and Lmax," Please give the Lmin and Lmax

directly in the figure.

[Response] Comments accepted. We have added "L_{min}" and "L_{max}" in Fig. 1a (Lines 683-685).

(2) Is there any reference for the conceptual representation of "REV curve" in L50?

[Response] Comments accepted. We have added reference for "REV curve" (Lines 52-53).

(3) L142. "Fig. 1c" should be "Fig. 1d".

[Response] Comments accepted. We have made corresponding correction (Line 152).

(4) L148. What does "n" mean in the Equation 5? And, the porosity does not occur in the Equation, how do you derive the porosity from it?

[Response] Comments accepted. We have replaced 'n' with 'θ' (Lines 53 and 158).

(5) L218-220. What is the difference between the and? Are they the same?

[Response] Comments accepted. We have corrected the sub and sup i (Line 256).

(6) The author should proofread the paper carefully, as the current paper has numerous typos.

For example,

L243: "Figure 2c" cannot be found in the paper.

L358, "All mean REV sizes of these variables for Experiment-II are larger than REVs of Experiments-II".

L386-387, the sentence does not have verb.

[Response] Comments accepted. We have checked carefully and corrected these mistakes above (Lines 180, 402 and 431-433).

A new criterion for determining the representative elementary volume of translucent porous media and inner contaminant

Ming Wu[1, 2], Jianfeng Wu[2*], Jichun Wu[2], and Bill X. Hu[1*]

[1] Institute of Groundwater and Earth Sciences, Jinan University, Guangzhou 510632, China

[2] Key Laboratory of Surficial Geochemistry, Ministry of Education; Department of Hydrosciences, School of Earth Sciences and Engineering, Nanjing University, Nanjing 210023, China

Correspondence to: J.F. Wu (jfwu@nju.edu.cn), B.X. Hu (billhu@jnu.edu.cn)

ABSTRACT

Representative elementary volume (REV) is essential to measure and quantify the effective parameters of a complex heterogeneous medium. To overcome the limitations of the existing REV estimation criteria~~Since previous REV estimation criteria having multiple limitations~~, a new REV estimation criterion (χ^i) based on dimensionless range and gradient calculation is proposed in this study to estimate REV of a translucent material based on light transmission techniques. ~~Two~~ Three sandbox experiments are performed to estimate REVs of porosity, density, tortuosity and perchloroethylene (PCE) plume using multiple REV estimation criteria. In comparison with χ^i, previous REV estimation criteria based on the coefficient of variation (~~C_V^i~~ C_V^i), the entropy dimension (DI^i ~~DI^i~~) and the relative gradient error (ε_g^i ~~ε_g^i~~) are tested in REV quantification of translucent silica and inner PCE plume to achieve their corresponding effects. Results suggest that new criterion (χ^i) can effectively identify the REV in the materials, whereas the coefficient of variation ~~(C_V^i)~~ and entropy dimension (DI^i) ~~cannot~~are not effective. The relative gradient error ~~(ε_g^i)~~ can make the REV plateau obvious, while random fluctuations make the REV plateau uneasy to identify accurately. Therefore, the new criterion is appropriate for REV estimation ~~for~~ of the translucent materials and inner contaminant. Models are built based on Gaussian equation to simulate the distribution of REVs for media properties, which frequency of REV is dense in the middle and sparse on both sides. REV estimation of PCE plume indicates high level of porosity lead to large value of mean and standard deviation for REVs of PCE saturation (S_o) and PCE-water interfacial area (A_{OW}). Fitted equations are derived from~~for~~ distribution of REVs for PCE plume related to d_m (distances from mass center to considered

point) and d_I (distances from injection position to considered point). Moreover, relationships between REVs of PCE plume and S_o are fitted using regression analysis. Results suggest a decreasing trend appears for S_o-REV when S_o increases, while A_{ow}-REV increases with increasing of S_o.

Keywords: new criterion; representative elementary volume (REV); translucent material

1. Introduction

Modelling groundwater and contaminant (such as hazardous irons) transport in subsurface environment is based on the premise that micro-structure of aquifer exist a representative elementary volume (REV) (Wang et al., 2016; Lei and Shi, 2019). REV acts as a micro-scale characteristic, which is important to improve our understanding of materials, inner fluid flow and other processes (Brown and Hsieh, 2000; Costanza-Robinson et al., 2011; Wu et al., 2017). Previous studies suggested that even the Platinum-Nanoparticle-Catalyzed hydrogenation reactions and ion transport through angstrom-scale slits in cell activity existed apparent size effect, implying size effect is a wide characteristic for many process and materials (Bai et al., 2016; Esfandiar et al., 2017). With the help of REV, a porous medium can be treated as continuum medium (Brown and Hsieh, 2000; Kang et al., 2003; Müller and Siegesmund, 2010; Teruel and Rizwan-uddin, 2010; Hendrick et al., 2012; Wang et al., 2012; Ukrainczyk and Koenders, 2014; Kim and Mohanty, 2016; Gilevska et al., 2019). A conceptual representation of "REV curve" (Brown and Hsieh, 2000), characterizing porosity ($n\theta$) change with measured scale (L) increment, is presented in Fig. 1ea. Based on the characteristic of REV curve in Fig. 1ae, the REV curve can be divided into three regions. When measured scale (Fig. 1b) is in region I, the porosity fluctuates drastically at small scales. As measured scale size ranging between L_{min} and L_{max}, a flat plateau with constant and steady value is encountered and the property is factored into its average value. Material property in spatial scales less than L_{min} is spatially varied portions with small scale, which can be easily influenced by individual pores in micro-structure such as region I (Fig. 1ca). Likewise, material property is allowed drift to new values in spatial scale above L_{max} due to additional morphological structures of large field heterogeneity (region III). As a matter of fact, REV scale of region II can be derived between the small and spatially varied property in region I and large field variability in region III. However, the lower and upper boundaries L_{min} and L_{max} of REV plateau is hard to be identified in reality (Brown and Hsieh, 2000; Costanza-Robinson et al., 2011).

As technology advanced and progressed, non-destructive and non-invasive techniques of x-ray and gamma ray micro-tomography were utilized for micro-structure characteristic measurement in materials (Ghilardi, 1993; Brown and Hsieh, 2000; Niemet and Selker, 2001; Bob et al., 2008; Al-Raoush and Papadopoulos, 2010; Costanza-Robinson et al., 2011; Al-Raoush, 2012; Borges and Pires, 2012; Fernandes et al., 2012; Rozenbaum and Roscoat, 2014; Pereira Nunes et al., 2016; Piccoli et al., 2019). Generally, REV estimation for material properties, inner gas and fluid also was usually implemented by micro visualization and scanning of X-ray and gramma ray in laboratory (Brown and Hsieh, 2000; Razavi et al., 2007; Nordahl and Ringrose, 2008; Al-Raoush and Papadopoulos, 2010; Costanza-Robinson et al., 2011; Rozenbaum and Roscoat, 2014; Borges et al., 2018), while different criteria were utilized to quantify REV (Brown and Hsieh, 2000; Martínez et al., 2007; Nordahl and Ringrose, 2008; Costanza-Robinson et al., 2011). Lower boundary scale L_{min}

of REV was identified by means of entropy dimension (DI^i DI^i) for eight soil samples (Martínez et al., 2007). Further, REV scale of permeability for ripple laminated sandstone intercalated with mudstone was estimated using the coefficient of variation (C_V^i C_V^i), which the REV scale is identified by the variability among the ten samples to achieve average REV scale (Nordahl and Ringrose, 2008). As a result, only one REV boundary was identified and not every sample can be estimated effectively (Nordahl and Ringrose, 2008). More interestingly, REV scales forof material property (porosity), moisture saturation and air-water interfacial areas in porous media were estimated by a criterion named the relative gradient error (ε_g^i)(Costanza-Robinson et al., 2011). REVs of permeability of translucent material, PCE saturation and PCE-water interfacial area also can be estimated using the relative gradient error (Wu et al., 2017). In summary, the REV estimation was made by multiple kinds of criteria, while the REV identification effects of these criteria were not clear. What's more, these previous criteria estimate REV scale unsatisfactorily that beginning and ending of REV plateau can't be identified simultaneously for translucent porous media based on light transmission technique. Therefore, new criterion which can identify REV plateau accurately is needed.

In this study, a new criterion (χ^i) for REV estimation is proposed to identify the REV scale of the translucent silica and inner contaminant. Two Three perchloroethylene (PCE) transport experiments are conducted in two dimensional (2D) sandboxes to test the effect of different REV estimation criteria. Translucent silica is selected for associated REV analysis due to its extensive utilization in laboratory experiment of exploring groundwater flow and contaminant migration behavior in micro-structure of a sandy aquifer (Niemet and Selker, 2001; Bob et al., 2008; Costanza-Robinson et al., 2011). Moreover, translucent silica is also an important material applied in numerous industries (Bouvry et al., 2016). In laboratory experiments, translucent silica is packed in 2D sandboxes where porosity, density, tortuosity~~,~~ and PCE saturation are derived by light transmission technique (Fig. 1c~~a~~). Porosity and PCE saturation are selected as the representative variables to explore corresponding REV estimation by different criteria, which is very essential and significant for REV identification. Previous criteria such as the coefficient of variation (C_V^i ~~C_V^i~~), entropy dimension (DI^i ~~DI^i~~), the relative gradient error (ε_g^i ~~ε_g^i~~) and the new criterion-χ^i are tested in REV estimation. Associated effects are analyzed to achieve the best criterion of effective and appropriate quantification of REV.

2. Experiment procedure and method

2.1 Experiment

~~Two~~ Three sandboxes (Fig. 2a-c ~~and b~~) packed by translucent silica medium are prepared in laboratory to test different criteria of REV quantification. PCE is selected as a typical DNAPL contaminant used in experiments. 2D sandbox is composed by three aluminum interior frames and two glass walls, which thickness is 1.6cm. The dimensions of sandboxes used in Experiment~~s~~-I ~~and II~~ are 20 (width) ×15 (height), and the dimensions of Experiments-II and III ~~and~~ are 60 (width) ×45 (height). F40/50 and F20/30 mesh translucent silica sands are used for background material for Experiments-I and II, while heterogeneous translucent silica with low porosity and permeability are packed in sandbox for Experiment-III. To make the translucent silica fully saturated by water in a flow field close to natural groundwater environment (Erning et al., 2012), water flow at flow velocity of 0.5 m/d is set from left to right in laboratory sandbox experiments (Fig. 2a-c and b). Water is restricted in a sandbox that the top and bottom layers of the sandbox are packed by F70/80 mesh translucent silica as capillary barriers. Light source is placed behind the sandbox to make light penetrate through translucent media and capture emergent light intensity using a thermoelectrically air-cooled charge-coupled device (CCD) camera (Fig. 1ca). Afterward, PCE is injected into sandboxes from the injection needle at constant rate of 0.5 mL /min for two three experiments. Detailed experimental conditions are listed in Table 1.

2.2 Light transmission techniques

By means of light transmission technique (Fig. 1ca), DNAPL and water saturation can be obtained rapidly and in real-time, which greatly help to explore the mechanism of groundwater flow and contaminant migration in porous media. When light passes through translucent materials of a given thickness, the emergent light intensity after the absorptive and interfacial losses can be expressed as (Niemet and Selker, 2001; Bob et al., 2008; Wu et al., 2017):

$$I_T = CI_0(\prod \tau_j)exp(-\sum \alpha_i d_i) \quad I_T = CI_0(\prod \tau_b)\exp(-\sum \alpha_a d_a) \tag{1}$$

where a represents phase number; b represent the number of the interface between phase a and a+1; I_0 is the original light intensity; C is a constant of correction for light emission and light observation; τ_{jb} is the transmittance when light penetrate from phase i a to a i+1; α_{ia} is the absorption coefficient when light penetrate in phase i a; d_{ia} is the length of light penetration path in phase i a.

To derive the porosity, the 2D translucent porous medium should be only saturated by water. Consequently, the emergent light intensity can be expressed as (Niemet and

Selker, 2001; Bob et al., 2008; Wu et al., 2017):

$$I_s = CI_0 \tau_{s,w}^{2k_o} \exp(-\alpha_s k_s d_s) \tag{2}$$

where $\tau_{s,w}^{2k_0}$ is the transmittance of solid-water interface; α_s is solid particles absorption coefficient; d_s is median diameter of the solid particles; k_o is the number of pores across light penetration path; k_s is the number of solid particles across light penetration path.

If we arbitrarily select an infinitesimal element, its area A_o approaches zero ($A_o \rightarrow 0$) from the 2D translucent porous media (Fig. 1d~~b~~), and suppose the infinitesimal element with thickness L_T containing solid particles and pores that can be regarded as lamellar structure (Fig. 1d~~e~~), we can obtain the following relationships (Wu et al., 2017):

$$\theta A_o L_T = A_o k_o d_o \tag{3}$$

$$k_s d_s + k_o d_o = L_T \tag{4}$$

where d_o is the median diameter of pores; θ is porosity.

Substituting Eq. (3) and Eq. (4) into Eq. (2), the relationship between emergent light intensity and porosity can be achieved (Wu et al., 2017):

~~$lnI_s = \beta + n\gamma$~~ $$lnI_s = \beta + \theta\gamma \tag{5}$$

where $\beta = \ln(\frac{CI_s}{e^{\alpha_s d_s L_T}})$ and $\gamma = \ln(\tau_{s,w}^{\frac{2L_T}{d_0}} e^{\alpha_s L_T})$ ~~$\gamma = \ln(\tau_{s,w}^{\frac{2L_s}{d_o}} e^{\alpha_s L_T})$~~ . β and γ can be determined from experimental data, then porosity can be obtained.

The density and tortuosity are derived as (Wu et al., 2018):

$$\rho = \theta\rho_w + (1.0 - \theta)\rho_s \tag{6}$$

$$\tau = 1 + \frac{\pi - 2}{\sqrt{\frac{\pi}{1-\theta}}} \tag{7}$$

where ρ is the density of translucent porous media; ρ_w is the density of water; ρ_s is the density of solid particles; τ is tortuosity.

The saturation of dense nonaqueous phase liquid (DNAPL) was quantified by light transmission technique based on light pass through translucent materials (Niemet and Selker, 2001; Bob et al., 2008):

$$S_o = \frac{\ln I_s - \ln I_T}{\ln I_s - \ln I_{oil}} \quad (8)$$

where S_o is the saturation of DNAPL; I_s is the light intensity after light penetration through translucent porous when all pores are fully saturated by water; I_{oil} is the light intensity when all pores are fully saturated by DNAPL; I_T is the light intensity after penetration through translucent materials. After quantification of PCE saturation, PCE-water interfacial area (A_{OW}) can be obtained based on the method proposed by Wu et al. (2017), where the unit of A_{OW} is cm^{-1}.

Emergent light intensity for three experiments is captured by a thermoelectrically air-cooled charge-coupled device (CCD) camera (Niemet and Selker, 2001; Bob et al., 2008). Every pixel with small scale could be approximated as infinitesimal element in high resolution image to apply light transmission techniques. As consequence, porosity of translucent silica was derived using light transmission technique through Eq. (5). The whole 2D translucent silica area was numerically discretized that every cell had the uniform dimensions of 0.015m×0.015m. The cuboid window (Fig. 1b) was utilized to quantify the variables (porosity, density, tortuosity, PCE saturation, PCE-water interfacial area) of every cell as measured scale was increased. In detail, the measured cuboid window scale was increased from the center of each cell and associated value of variable was calculated from the high resolution porosity of 2D translucent silica derived by light transmission technique.

Observation cells were selected from the discretized cells (Fig. 3b) of which the cells I-1~2, II-1~2 and III-1~2 belong to Experiments-I-III, respectively.

To analyze the regularity of REV distribution for PCE plume, the mass center coordinate and the granglia-to-pool ratio (GTP) of PCE plume are quantified for Experiments-I-III. The mass center coordinate and GTP are calculated as:

$$X_m = \frac{M_{10}}{M_{00}} \quad (9)$$

$$Z_m = \frac{M_{01}}{M_{00}} \quad (10)$$

$$GTP = \frac{V_{ganglia}}{V_{pool}} \quad (11)$$

where X_m is x coordinate of mass center for PCE plume; Z_m is z coordinate of mass center for PCE plume; GTP is granglia-to-pool ratio, which equals to the ratio of the $V_{ganglia}$ to V_{pool}; $V_{ganglia}$ is the PCE volume under ganglia state; V_{pool} is the PCE volume under pool state; M_{00}, M_{10} and M_{01} are computed using definition of spatial moment (M_{ij}), $M_{ij} = \int_{x_0}^{x_1}\int_{z_0}^{z_1} \theta(x,z) S_o(x,z,t) x^i z^j d_x d_z$; x_0 and z_0 are minimum limits of x axis and z axis; x_1 and z_1 are maximum limits of x axis and z axis; θ(x,z) is the porosity at point (x,z); $S_o(x,z,t)$ is PCE saturation of point (x, z) at time t.

2.3 Criteria of REV quantification

The REV is defined as the volume range in which all material characteristics are factored into the average and associated values approach single and constant (Brown and Hsieh~~s~~, 2000). In the range of REV, the value of one associated property will meet the condition:

$$\frac{\partial Y(L_i)}{\partial L}\Big|_{L_i=L_o} = 0 \quad (12~~9~~)$$

where the Y(L_i) is the value of an associated property when system scale is L_i; L_i is the value of system scale; L_o is the scale range of REV, $L_{min}<L_o<L_{max}$; L_{max} is upper boundary of REV; L_{min} is lower boundary of REV scale. According to the Eq. (129), when the measured scale (L_i) reaches REV range, the derivative $\frac{\partial Y(L_i)}{\partial L} \rightarrow 0$ $\frac{\partial Y(L_i)}{\partial L} \rightarrow 0$ will tend to zero. As a matter of fact, most previously used criteria were applied to estimate REV based on this requirement. The REV estimation criteria tested in this study are illustrated in Table 2 (Brown and Hsieh, 2000; Martínez et al., 2007; Nordahl and Ringrose, 2008; Costanza-Robinson et al., 2011).

To evaluate the REV of porosity, the coefficient of variation (C_V^i C_V^i) (Table 2) is utilized to estimate the variability (Nordahl and Ringrose, 2008):

$$C_V^i = \frac{\hat{s}_i}{\overline{\varphi}_i} \quad C_V^i = \frac{\hat{s}_i}{\overline{\varphi}_i} \tag{130}$$

where i is the cuboid window (Fig. 1bb) increment number; φ φ is the measured variable, such as porosity; $\hat{s}_i$ $\hat{s}_i$ is the standard deviation of sub-grids' variable in different measured volume or scale; $\overline{\varphi}_i$ $\overline{\varphi}_i$ is the arithmetic average of the variable values in the sub-grids. When number of sub-grids (N) is less than 10, a correction is utilized to replace Eq. (130). According to Nordahl and Ringrose (2008), $0 < C_V^i < 0.5$ $0 < C_V^i < 0.5$ is defined as homogeneous and $C_V^i = 0.5$ $C_V^i = 0.5$ can be used as criterion to identify the REV scale.

Similarly, for porosity of translucent silica, entropy dimension (DI^i) (Table 2) is utilized for REV analysis and estimation (Martínez et al., 2007), which is defined as:

$$DI^i \approx \frac{\sum_{j=1}^{m(i)} \mu_j(L_\varepsilon) \log \mu_j(L_\varepsilon)}{\log L_\varepsilon} \tag{141}$$

where, L_ε is the scale of sub-grid; "≈" indicates the asymptotic equivalence as $L_\varepsilon \rightarrow 0$ (Martínez et al., 2007); j is the ordinal number of sub-grid in measured cuboid window (Fig. 1b~~b~~) of increment number i; $m(i)$ is the total number of sub-grids in measured cuboid window (Fig. 1b~~b~~) of increment number i; $\mu_j(\varepsilon)$ ~~$\mu_j(\varepsilon)$~~ is the proportion of the variable of sub-grid j in the whole measured cuboid window i. The right hand side of Eq. (14~~1~~) is the simplification of Shannon entropy of all sub-grids, in which DI^i ~~DI^i~~ can be considered as the average of logarithmic values of the variable distribution weighted by $\mu_j(L_\varepsilon)$ ~~$\mu_j(L_\varepsilon)$~~ to quantify the degree of medium heterogeneity. Using Eq. (14~~1~~), a series of values of DI^i ~~DI^i~~ (i=1,2,3…) are obtained for each measured cuboid window (Fig. 1b) of increment number i. For estimation of the REV in a porous medium, the relative increment of entropy dimension and associated criterion of REV identification are respectively expressed as:

$$RI^i = \left| \frac{DI^j - DI^{j-1}}{DI^{j-1}} \right| \times 100 \qquad \text{~~} RI^i = \left| \frac{DI^j - DI^{j-1}}{DI^{j-1}} \right| \times 100 \text{~~} \tag{15~~2~~}$$

$$RI^i \leqslant 0.2 CV_{DI} \tag{16~~3~~}$$

where CV_{DI} ~~CV_{DI}~~ is the coefficient of variation of DI^i ~~DI^i~~ series (i=1,2,3…), which is calculated through $CV_{DI} = (\hat{s}_{DI}/\overline{DI}) \times 100$ ~~$CV_{DI} = (\hat{s}_{DI}/\overline{DI}) \times 100$~~; $\overline{DI}$ ~~$\overline{DI}$~~ is the mean value of the DI^i ~~DI^i~~ series; $\hat{s}_{DI}$ ~~$\hat{s}_{DI}$~~ is the standard deviation of the DI^i ~~DI^i~~ series.

To achieve the REV for multiple system variables, such as porosity, moisture saturation and air-water interfacial areas in an unsaturated porous medium, a criterion named the relative gradient error ~~(Table 2)~~ was applied (Costanza-Robinson et al., 2011):

$$\varepsilon_g^i = \left| \frac{\varphi^{i+1} - \varphi^{i-1}}{\varphi^{i+1} + \varphi^{i-1}} \right| \frac{1}{\Delta L} \qquad \text{~~} \varepsilon_g^i = \left| \frac{\varphi^{i+1} - \varphi^{i-1}}{\varphi^{i+1} + \varphi^{i-1}} \right| \frac{1}{\Delta L} \text{~~} \tag{17~~4~~}$$

where ε_g^i ~~ε_g^i~~ is relative gradient error; ΔL is the measured cuboid window size increment length for REV estimation. Usually, ε_g^i ~~ε_g^i~~ less than 0.2 (Costanza-Robinson et al., 2011) is utilized to identify a REV sizes.

According to the requirement in Eq. (12), a~~A~~ new criterion based on the required condition of REV is proposed to estimate the REV range ~~for~~ of the translucent silica in this study:

~~$$\chi^i = \frac{|\delta_{i+1} - \delta_{i-1}|}{\delta_i \Delta L}$$~~ ~~$$\chi^i = \frac{|\delta^{i+1} - \delta^{i-1}|}{\delta^i \Delta L}$$~~ $$\chi^i = \frac{|\delta^{i+1} - \delta^{i-1}|}{\delta^i \Delta L} \qquad (18~~5~~)$$

where δ^i ~~δ^i~~ is the dimensionless range, $\delta^i = \frac{\varphi(L_i)_{max} - \varphi(L_i)_{min}}{\overline{\varphi(L_i)}}$ ~~$\delta^i = \frac{\phi(L_i)_{max} - \phi(L_i)_{min}}{\overline{\phi(L_i)}}$~~; $\varphi(L_i)_{max}$ ~~$\varphi(L_i)_{max}$~~ is the maximum value of the variable on the volume scale L_i; $\varphi(L_i)_{min}$ ~~$\varphi(L_i)_{min}$~~ is the minimum value of the variable on the volume scale L_i; $\overline{\varphi(L_i)}$ ~~$\overline{\varphi(L_i)}$~~ is the mean value of the variable on the volume scale L_i. Brown and Hsieh (2000) suggested $\delta^i = \frac{\varphi(L_i)_{max} - \varphi(L_i)_{min}}{\overline{\varphi(L_i)}} << 1$ ~~$\delta^i = \frac{\phi(L_i)_{max} - \phi(L_i)_{min}}{\phi(L_i)} << 1$~~ can be used for REV estimation. In fact, the calculated value of δ^i ~~δ^i~~ mostly is less than 1, while $\delta^i << 1$ ~~$\delta^i << 1$~~ is hard to be used to identify the REV scale for realistic materials, such as the translucent silica used in this study. The value limit of χ^i used for REV estimation also is explored in this study.

In this study, criteria for the coefficient of variation (C_V^i ~~C_V^i~~), entropy dimension (DI^i ~~DI^i~~), the relative gradient error (ε_g^i ~~ε_g^i~~) and the new criterion (χ^i) are all applied to~~in~~ REV estimation for porosity and PCE saturation. Corresponding REV plateau identification effects are compared to select the best criterion for REV quantification.

3. Results and discussion

3.1 REV identification effect of different criteria

3.1.1 The coefficient of variation

Emergent light intensity distributions of translucent silica for ~~two~~ three experiments, which had been fully saturated by water, ~~was~~ were obtained by a thermoelectrically air-cooled ~~charge-coupled device (~~CCD~~)~~ camera (Niemet and Selker, 2001; Bob et al., 2008). The porosity, density, tortuosity and PCE saturation for ~~two~~ three experiments are derived by light transmission technique as shown in Figs. 3a and b. The PCE spreads from the injecting point shaped like a drop of water at t=~~1.44~~5 min (Fig. 3b). In 2D sandboxes for ~~two~~ three experiments, PCE plume infiltrates in translucent silica sands~~ infiltration paths~~ and~~ PCE plumes~~ reaches the bottom after t=80 min.

~~Every pixel with small scale could be approximated as infinitesimal element in high resolution image to apply light transmission techniques. As consequence, porosity of translucent silica was derived with light transmission technique through Eq. (5) (Fig. 2c). The whole 2D translucent silica area was numerically discretized that every cell had the uniform dimensions of 0.015m×0.015m. The cuboid window (Fig. 1bd) was utilized to quantify the variables (porosity, density, tortuosity, PCE saturation, PCE-water interfacial area) of every cell as measured scale was increased. In detail, the measured cuboid window scale was increased from the center of each cell and associated value of variable was calculated from the high resolution porosity of 2D translucent silica derived by light transmission technique. Observation cells were selected from the discretized cells (Fig. 3b) of which the cells I-1~2 and II-1~2 belong to Experiments I and II, respectively.~~ Porosity and PCE saturation variation curves of these all observation cells with increasing measured cuboid window scale were shown in Figs. 4a and b. However, for all observation cells from translucent silica, the REV plateaus were not obvious to be objectively judged visually, which made REV plateaus hard to identify effectively by original variation curves for porosity and PCE saturation (Figs. 4a and b).

To make the REV plateau more explicit, different criteria of REV quantification are utilized. The coefficient of variation (C_V^i C_V^i) of porosity and PCE saturation fluctuating with increasinge of measured cuboid window size is shown in Fig. 4. The measured cuboid window scale is limited to the dimensions of cells in discretization of 2D translucent silica. The observation cells show various characteristics of variation tendency for the coefficient of variation (C_V^i C_V^i). The θ and S_o variation curves of the coefficient of variation (C_V^i) for all observation cells do not reach stable values as those shown in Figs. 4a and b, the beginning of the REV flat plateau is not easy to identify, the coefficient of variation (C_V^i C_V^i) is not suitable for REV estimation. According to the heterogeneity definition by Corbett and Jensen (1992), the heterogeneity of materials is defined by C_V^i C_V^i magnitude that $0 < C_V^i < 0.5$ $0 < C_V^i < 0.5$ is classed as homogeneous medium, $0.5 < C_V^i < 1.0$ $0.5 < C_V^i < 1.0$ is classed as heterogeneous medium and $1.0 < C_V^i$ $1.0 < C_V^i$ is classed as strong heterogeneous medium. For the coefficient of variation (C_V^i C_V^i) magnitude in Figs. 4a and b f, the C_V^i C_V^i values are all below 0.5 that the criterion $C_V^i = 0.5$ $C_V^i = 0.5$ is unable to identify the REV scale for translucent silica.

3.1.2 Entropy dimension

Entropy dimension (DI^i) is utilized by Martínez et al. (2007) for multifractal analysis of a porous medium porosity and REV estimation. In this study, entropy dimension (DI^i ~~DI^i~~) is tested to avoid unclear REV plateau in porosity curves. The entropy dimension (DI^i ~~DI^i~~) of porosity is calculated by Eq. (14~~1~~). Variation curves of entropy dimension (DI^i ~~DI^i~~) for all observation cells (Fig. 2a) are presented in Fig. 4. The curves of entropy dimension (DI^i ~~DI^i~~) of porosity and PCE saturation generally result in the increasing trend curves which makes REV estimates become very difficult and invalid. Entropy dimension (DI^i ~~DI^i~~) was quickly increased with increasing of measured cuboid window size. Compared to the coefficient of variation (C_V^i ~~C_V^i~~) of porosity and PCE saturation, entropy dimension (DI^i ~~DI^i~~) increased step by step without opposite fluctuation tendency in the variation curves as the length scale of measured cuboid window increased simultaneously. In general, REV plateau in region II (Fig. 1a~~e~~) of porosity is not obvious for the entropy dimension (DI^i ~~DI^i~~) curves of all observation cells from ~~two~~ three experiments, which suggests REV scales is uneasy to identify for translucent silica using entropy dimension (DI^i ~~DI^i~~) by light transmission technique.

3.1.3 The relative gradient error

The relative gradient error (ε_g^i ~~ε_g^i~~) of porosity and PCE saturation is calculated by Eq. (17~~4~~). The variation of ε_g^i ~~ε_g^i~~ at different measured cuboid window scales ~~are~~ is shown in Fig. 4 for all observation cells in the 2D translucent silica. For all ε_g^i ~~ε_g^i~~ curves at observation cells from experiments, the REV plateaus in region II (Fig. 1a) are more clear than the variation curves based on the criteria of C_V^i ~~C_V^i~~ and DI^i ~~DI^i~~. Apparently, erratic variations of the relative gradient error (ε_g^i ~~ε_g^i~~) at small measured cuboid window scales are observed for all ε_g^i ~~ε_g^i~~ curves as the characteristic of REV region I in Fig. 1a~~e~~. When measured cuboid window scale further increases for all observation cells, the variability and magnitude of the relative gradient error (ε_g^i ~~ε_g^i~~) decrease well and factor~~ed~~ into average, which can be identified as REV plateau in region II (Fig. 1a~~e~~). The relative gradient error (ε_g^i ~~ε_g^i~~) makes the REV plateau quantification convenient for all observation cells. At the measured cuboid window size above the REV plateau, ε_g^i ~~ε_g^i~~ curves result in large variability for observation cells I-1~2. These findings suggest that that the relative gradient error (ε_g^i ~~ε_g^i~~) can make the REV plateau more obvious, which greatly contribute to convenient and applicable REV quantification for translucent silica by light transmission technique. However, random fluctuations exist in ε_g^i ~~ε_g^i~~ curves visually, which make the REV plateau uneasy to identify accurately.

3.1.4 The new criterion (χ^i)

χ^i of porosity and PCE saturation changing with measured cuboid window size is shown in Fig. 4. Like the region I (Fig. 1a~~e~~), erratic and random fluctuations appear~~s~~ at small measured cuboid window sizes and χ^i increases with the increase of the measured cuboid window size. When measured scale increases, the values of χ^i for all observation cells appear fast reduction and rapidly tend to steady, which exhibit the characteristic of REV plateau as measured scale reaches region II. The χ^i for observation cells restores the erratic variation state of increasing trend after measured cuboid window size exceeding the REV plateau. As shown in the variation curves of χ^i for all observation cells, the beginning of the REV flat plateaus can be identified easily, suggesting χ^i is more convenient and reliable than other methods for REV estimation. All observation cells show similar variation curves of χ^i that low value intervals are quite apparent, indicating that χ^i is very effective to make the REV plateau obvious for translucent silica used in this study. Using the criterion of χ^i, the REV plateau of region II is flat, which is easily identified, compared with other criteria for observation cells (Figs. 4a and b).

3.2 REVs of material properties

Based on the REV plateau identifications using the coefficient of variation (C_V^i ~~C_V^i~~),entropy dimension (DI^i ~~DI^i~~), the relative gradient error (ε_g^i ~~ε_g^i~~) and the proposed new criterion χ^i in Figs. 4a and b, the new criterion χ^i appears to be the most appropriate criterion for REV plateau identification. Even though the relative gradient error (ε_g^i ~~ε_g^i~~) can also make REV plateau obvious, but various random fluctuations weaken the method and reduce the associated accuracy. Therefore, REVs of porosity, density, tortuosity and PCE plume are estimated using the new criterion χ^i in the following study.

In fact, large number of discretized cells in the 2D translucent silica for ~~two~~ three experiments are quantified using the new criterion χ^i, which is convenient to examine the regularities for REV sizes and related factors. Using the new criterion χ^i, the REV estimation is conducted based on Eq. (1~~5~~8). Fig. 5a shows minimum REV sizes of porosity, density and tortuosity quantified by χ^i for all cells of ~~two~~ three experiments. Associated statistical analysis for REVs is illustrated in Fig. 5b, where circular points represent frequency and triangular points represent cumulative frequency. Frequency of REVs is dense in the middle and sparse on both sides, so the distribution of REVs can be fitted by Gaussian equation:

$$~~F = \omega + \frac{1}{\sqrt{2\pi}\delta} e^{-\frac{(\mathrm{REV}-\nu)}{2\delta^2}}~~ \quad F = \omega + \frac{1}{\sqrt{2\pi}\epsilon} e^{-\frac{(REV-\nu)^2}{2\epsilon^2}} \qquad (19~~6~~)$$

where F is the frequency of REV; ω, ~~δ~~ ~~ε~~ ϵ and ν are fitted parameters of the model.

After regression analysis, the derived models for REV frequency are listed in Table ~~3~~2. The coefficients of determination (R^2) of models for REVs of porosity and density for three experiments all exceed 0.85~~93~~. R^2 for REV of tortuosity for ~~two~~ three experiments exceeds 0.76. Moreover, the computed cumulative frequency based on models fit cumulative frequency from experimental results well in Fig. 5b.

The minimum REV size frequency ~~for~~ of porosity appears a peak between 4.0 mm and 5.0 mm for Experiment-I. As minimum REV size of porosity increases, corresponding frequency continuously decreases. Further, smooth convex shape of cumulative frequency is observed for minimum REV size of porosity (Fig. 5b). Most minimum REV sizes of translucent silica distributed in 0.0-7.0mm. For density of translucent silica sand, associated REV frequency appears high values between 2.0~3.0 mm. For the REV sizes of tortuosity, minimum REV sizes distribute in 0.0~6.0 mm. Compared with Experiment-I (F40/50 mesh translucent silica sand), the frequency of REV for Experiment-II (F20/30 mesh translucent silica sand with larger porosity) shows flat shape and has larger value of standard deviation, especially for REV of porosity. Fig. 5b shows that translucent silica with larger porosity will achieve border distribution of minimum REV sizes distribution compared to translucent silica with relative lower porosity. Moreover, the frequency of REV of porosity and permeability for Experiment-III (background material is F20/30 mesh translucent silica sand with larger porosity, five lenses with lower porosity is packed in sandbox to create heterogeneity) is similar to the frequency of REV for Experiment-II. However, the frequency of τ-REV for Experiment-III is different from the frequency of τ-REV for Experiment-II under homogeneous condition. The mean REV sizes of porosity, density and tortuosity for Experiment-I are 4.35 mm, 2.89 mm and 3.65 mm, respectively. All mean REV sizes of these variables for Experiment-II are larger than REVs of Experiments-I~~I~~, which corresponding mean REV sizes are 8.05 mm, 2.97 mm and 4.30 mm. These results suggest translucent porous media with higher porosity lead to larger values of mean and standard deviation for REV sizes.

3.3 REVs of S_o and A_{OW} for PCE plume

Based on the new criterion χ^i and light transmission technique, the real-time distributions of S_o-REV and A_{OW}-REV for PCE plume can be obtained over the entire experimental period. The minimum REV sizes of S_o and A_{OW} obtained using new criterion χ^i are shown in Figs. 6a and b.~~–~~ When PCE migrates in sandbox, the REV of PCE plume is changed over time (Fig. 6). The REVs of PCE plume for Experiment-I mostly are lower than the REVs of PCE plume for Experiments-II and III. Moreover, when heterogeneous porous media is packed in sandbox, the REV distribution of Experiment-III become more heterogeneous compared with REV distribution of Experiments-II under homogeneous condition. Based on REV distributions of PCE plume for three experiments, statistical analysis is conducted to explore the regularity of REV distribution for PCE plume. ~~To analyze the regularity of REV distribution for PCE plume, the mass center coordinate of PCE plume for two experiments are quantified for Experiments-I and II. The mass center coordinate are calculated as:~~

~~$x_m = \frac{M_{10}}{M_{00}}$ (17)~~

~~$z_m = \frac{M_{01}}{M_{00}}$ (18)~~

~~where x_m is x coordinate of mass center for PCE plume; z_m is z coordinate of mass center for PCE plume; M_{00}, M_{10} and M_{01} are computed using definition of spatial moment (M_{ij}), $M_{ij} = \int_{x_0}^{x_1}\int_{z_0}^{z_1} \theta(x,z) S_o(x,z,t) x^i z^j d_x d_z$; x_0 and z_0 are minimum limits of x axis and z axis; x_1 and z_1 are maximum limits of x axis and z axis; θ(x,z) is the porosity at point (x,z); $S_o(x,z,t)$ is PCE saturation of point (x, z) at time t.~~

The mass center coordinate of PCE plume, GTP and plume area~~derived by Eq. (18)~~ are~~is~~ shown in Fig. 7a. The values of X_m, Z_m and GTP for Experiment-II and III are higher than the X_m, Z_m and GTP of Experiment-I (lower porosity). Moreover, the plume area of Experiment-II is larger than the plume of Experiment-I. When packed material is heterogeneous, the plume area of PCE is increased further for Experiment-III. Besides, the mean and standard deviation of REVs of PCE plume during 0~1523 min are derived by statistical analysis (Fig. 7a). Compared with REVs of PCE plume for Experiment-I, Experiment-II (F20/30 mesh translucent silica sand with higher porosity) has larger value of mean and standard deviation of REVs. The mean value of A_{OW}-REV for Experiment-III is much higher than A_{OW}-REV for Experiments-I and II.

~~Afterward, t~~The average value of REVs ($\overline{REV}$ ~~$\overline{\overline{REV}}$~~) and associated distance (d_m) from mass center to corresponding cells contained in PCE plume at t=1523 min are presented in Fig. 7b~~a~~. Regression analysis is performed for average REVs of PCE plume and d_m, where fitted models and associated R^2 for Experiments-I-III~~ and II~~ are listed in Table ~~4~~3.

Simultaneously, the fitted equations between $\overline{REV}$ $\overline{REV}$ and d_I (the distance from injection point to cell contained in PCE plume) also are derived by regression analysis. From the results in Fig. 7a, $\overline{REV}$ $\overline{REV}$ of S_o and A_{ow} appear a peak and then decrease with increasing of d_m and d_I for Experiment-I. $\overline{REV}$ $\overline{REV}$ of S_o and A_{ow} for Experiment-I all firstly increase and then decrease with the increasing of d_m and d_I,. Howeverwhile, $\overline{REV}$ $\overline{REV}$ of PCE plumeS_o presents apparent decreasing tendency as d_m and d_I increase for Experiment-II, and $\overline{REV}$ of A_{ow} just slightly increase first and then decrease for Experiment-II. In addition, the value of A_{OW}-REV mostly is higher than the value of S_o-REV for two three experiments. Compared with the R^2 of the fitted relationship between average REVs of PCE plume and d_m, d_I for Experiments-I and II, the values of R^2 achieved by Experiment-III are much lower (Table 3).

The mean and standard deviation of REVs of PCE plume during 0~1523 min derived by statistical analysis (Fig. 7b). Compared with REVs of PCE plume for Experiment-I, Experiment-II (F20/30 mesh translucent silica sand with higher porosity) has larger value of mean and standard deviation of REVs. Besides, the relationship between REVs and PCE saturation are fitted by regression analysis, where fitted equation and R^2 for two three experiments are listed in Table 45 and Fig. 7b. With increasing of PCE saturation, REV of S_o appear decline trend for two three experiments. However, REV of A_{OW} increases when S_o increases for both twoall three experiments (Fig. 7b). On the other hand, REV of S_o for Experiment-II is higher than corresponding REV for Experiment-I, while Experiments-I and II have similar values of A_{OW}-REV (Fig. 7b). Moreover, REVs of S_o and A_{OW} for Experiment-III are higher than REVs of S_o and A_{OW} for Experiments-I and II. These results suggest higher porosity will lead to high value of S_o-REV and the relationship between REVs of PCE plume and dm, d_I. S_o-REV and A_{OW}-REV are increased under heterogeneous condition.

4. Conclusions

In this study, a new criterion χ^i is proposed to identify the REVs of translucent porous media and inner contaminant transformation based on previous criteria. The REV plateaus of observation cells selected from ~~two~~ three experiments of PCE transport are hard to judge visually from the porosity and PCE saturation curves. From the REV identification effects of different criteria, the REV flat plateau is difficult to identify by the coefficient of variation (C_V^i ~~C_V^i~~) and entropy dimension (DI^i ~~DI^i~~), indicting the coefficient of variation (C_V^i ~~C_V^i~~) and entropy dimension (DI^i ~~DI^i~~) are not suitable for REV estimation of translucent porous media. The relative gradient error (ε_g^i ~~ε_g^i~~) can make REV plateaus of all kinds of translucent silica explicit in variation curves, but random fluctuations weaken REV plateau identification. In comparison with these previous criteria, the beginning and ending of the REV flat plateaus could be easily and directly identified in the curves based on the new criterion χ^i, suggesting the new criterion χ^i is more convenient and effective for REV estimation. In this study, REVs of porosity, density, tortuosity, and PCE plume are estimated using the new criterion χ^i.

Statistical results of minimum REV scales quantified by new criterion χ^i reveal cumulative frequencies of porosity, density and tortuosity all have smooth convex shapes. Models based on Gaussian equation are built for the distribution of REVs of porosity, density and tortuosity, which porous media with larger porosity leads to larger values of mean and standard deviation for REV sizes of media properties. For REVs of PCE plume, result suggested larger porosity lead to larger value of mean and standard deviation. Regression analysis is performed to study the regularity for distribution of REVs, where fitted relationship between REVs and d_m, d_I are derived for PCE plume. $\overline{REV}$ ~~$\overline{\mathrm{REV}}$~~ of S_o and A_{ow} firstly increase and then decrease with the increasing of d_m and d_I for Experiment-I whose sandbox packed by translucent porous media with relatively lower porosity. However, $\overline{REV}$ ~~$\overline{\mathrm{REV}}$~~ of S_o and A_{ow} directly decrease with the increment of d_m and d_I when porosity became larger for Experiment-II. The values of R^2 of the fitted relationship between average REVs of PCE plume and d_m, d_I for Experiment-III are much lower under heterogeneous condition. Significantly, REV size of S_o presented decreasing trend as S_o increases, while increasing tendency appeared for REV size of A_{ow}. Through regression analysis, the fitted equations between REVs of PCE plume and PCE saturation are derived for ~~two~~ three experiments. Implications of these finding are essential for quantitative investigation of scale effect of porous media and contaminant transformation. The fluid migration and transform in porous media can be simulated accurately according to the REV estimation results using light transmission technique and the appropriate criterion χ^i.

Code and data availability

The codes and data for this paper are available by contacting the corresponding author at jfwu@nju.edu.cn.

Author contributions

Ming Wu: Conceptualization, Methodology, Writing;

Jianfeng Wu: Conceptualization, Methodology, Writing;

Jichun Wu: Conceptualization;

Bill X. Hu: Conceptualization, Writing.

Declaration of interests

The authors declare that they have no known competing financial interests or personal relationships that could have appeared to influence the work reported in this paper.

Acknowledgments

We acknowledge support by the National Key Research and Development Plan of China (2019YFC1805302 and 2016YFC0402800), the National Natural Science Foundation of China (41902246, 41730856 and 41772254), the Natural Science Foundation of Guangdong Province (2020A1515010447) and~~,~~ the Fundamental Research Funds for the Central Universities (14380105)~~the National Natural Science Foundation of China-Xianjiang Project (U1503282) and the China Postdoctoral Science Foundation (2017M622905)~~.

References

Al-Raoush, R., and Papadopoulos, A.: Representative elementary volume analysis of porous media using X-ray computed tomography, Power Technol., 200, 60-77, 2010.

Al-Raoush, R.: Change in Microstructure Parameters of Porous Media Over Representative Elementary Volume for Porosity, Part. Sci. Technol., 30, 1-16, 2012.

Bai, L., Wang, X., Chen, Q., Ye, Y., Zheng, H., Guo, J., Yin, Y., and Gao, C.: Explaining the Size Dependence in Platinum-Nanoparticle-Catalyzed Hydrogenation Reactions, Angew. Chem. Int. Ed., 55, 15656-15661, 2016.

Bob, M.M., Brooks, M.C., Mravik, S.C., and Wood, A.L.: A modified light transmission visualization method for DNAPL saturation measurements in 2-D models, Adv. Water Resour., 31, 727-742, 2008.

Borges, J.A.R., and Pires, L.F.: Representative elementary area (REA) in soil bulk density measurements through gamma ray computed tomography, Soil Till. Res., 123, 43-49, 2012.

Borges, JAR., Pires, L.F., Cássaro, F.A.M., Roque, W.L., Heck, R.J., Rosa, J.A., and Wolf, F.G.: X-ray microtomography analysis of representative elementary volume (REV) of soil morphological and geometrical properties, Soil Till. Res., 182, 112-122, 2018.

Bouvry, B., del Campo, L., Meneses, D.D.S., Rozenbaum, O., Echegut, R., Lechevalier, D., Gaubil, M., and Echegut, P.: Hybrid methodology for retrieving thermal radiative properties of semi-transparent ceramics, J. Phys. Chem. C, 120, 3267-3274, 2016.

Bradford, S.A., Vendlinski, R.A., and Abriola, L.M.: The entrapment and long-term dissolution of tetrachloroethylene in fractional wettability porous media, Water Resour. Res., 35(10), 295-2964, 1999.

Brown, G.O., and Hsieh, H.T.: Evaluation of laboratory dolomite core sample size using

representative elementary volume concepts, Water Resour. Res., 36(5), 1199-1207, 2000.
Corbett, P.W.M., and Jensen, J.L.: Estimating the mean permeability: how many measurement do we need? First Break, 10(3), 89-94, 1992.
Costanza-Robinson, M.S., Estabrook, B.D., and Fouhey, D.F.: Representative elementary volume estimation for porosity, moisture saturation, and air-water interfacial areas in unsaturated porous media: Data quality implication, Water Resour. Res., 47, W07513, 2011.
Erning, K., Grandel, S., Dahmke, A., and Schäfe, D.: Simulation of DNAPL infiltration and spreading behavior in the saturated zone at varying flow velocities and alternating subsurface geometries, Environ. Earth Sci., 65, 1119-1131, 2012.
Esfandiar, A., Radha, B., Wang, F.C., Yang, Q., Hu, S., Garaj, S., Nair, R.R., Geim, A.K., and Gopinadhan, K.: Size effect in ion transport through angstrom-scale slits, Science, 358, 511-513, 2017.
Fernandes, J.S., Appoloni, C.R., and Fernandes, C.P.: Determination of the Representative Elementary Volume for the study of sandstones and siltstones by X-Ray microtomography, Mater. Res., 15(4), 662-670, 2012.
Ghilardi, P., Kai, A.K., and Menduni, G.: Self-similar heterogeneity in granular porous media at the representative elementary volume scale, Water Resour. Res., 29(4), 1205-1214, 1993.
Gilevska, T., Passeport, E., Shayan, M., Seger, E., Lutz, E.J., West, K.A., Morgan, S.A., Mack, E.E., and Lollar, B.S.: Determination of in situ biodegradation rates via a

novel high resolution isotopic approach in contaminated sediments, Water Res, 149, 632-639, 2019.

Hendrick, A.G., Erdmann, R.G., and Goodman, M.R.: Practical Considerations for Selection of Representative Elementary Volumes for Fluid Permeability in Fibrous Porous Media, Transp. Porous Med., 95, 389-405, 2012.

Kang, Q.J., Zhang, D.X., and Chen, S.Y.: Simulation of dissolution and precipitation in porous media, J. Geophys. Res. 108, NO. B10, 2505, doi:10.1029/2003JB002504, 2003.

Kim, J., and Mohanty, B.P.: Influence of lateral subsurface flow and connectivity on soil water storage in land surface modeling, J. Geophys. Res. Atmos., 121,704-721, 2016.

Lei, S., and Shi, Y.: Separate-phase model and its lattice Boltzmann algorithm for liquid-vapor two-phase flows in porous media, Phys. Rev. E, 99, 053302, 2019.

Martínez, F.S.J., Caniego, F.J., García-Gutiérrez, C., and Espejo, R.: Representative elementary area for multifractal analysis of soil porosity using entropy dimension, Nonlin. Processes Geophys., 14, 503-511, 2007.

Müller, C., and Siegesmund, S.: Evaluation of the representative elementary volume (REV) of a fractured geothermal sandstone reservoir, Environ. Earth Sci., 61, 1713-1724, 2010.

Niemet, M.R., and Selker, J.S.: A new method for quantification of liquid saturation in 2D translucent porous media systems using light transmission, Adv. Water Resour., 24, 651-666, 2001.

Nordahl, K., and Ringrose, P.S.: Identifying the Representative Elementary Volume for permeability in heterolithic deposits using numerical rock models, Math Geosci., 40, 753-771, 2008.

O'Carroll, D.M., Bradford, S.A., and Abriola, L.M.: Infiltration of PCE in a system containing spatial wettability variations, J. Contam. Hydrol., 73, 39-63, 2004.

Pereira Nunes, J.P., Blunt, M.J., and Bijeljic, B.: Pore-scale simulation of carbonate dissolution in micro-CT images, J. Geophys. Res. Solid Earth, 121, 558-576, 2016.

Piccoli, I, Schjønning, P., Lamandé, M., Zanini, F., and Morari, F.: Coupling gas transport measurements and X-ray tomography scans for multiscale analysis in silty soils, Geoderma, 338, 576-584, 2019.

Razavi, M.R., Muhunthan, B., and Al Hattamleh, O.: Representative elementary volume analysis of sands using x-ray computed tomography, Geotech. Test J., 30(3), 212-219, 2007.

Rozenbaum, O., and du Roscoat, S.R.: Representative elementary volume assessment of three-dimensional x-ray microtomography images of heterogeneous materials:Application to limestones, Phys. Rev. E, 89, 053304, 2014.

Teruel, F.E., and Rizwan-uddin: Numerical computation of macroscopic turbulence quantities in representative elementary volumes of the porous medium, Int. J. Heat Mass Transfer., 53, 5190-5198, 2010.

Ukrainczyk, N., and Koenders, E.A.B.: Representative elementary volumes for 3D modeling of mass transport in cementitious materials, Modelling Simul. Mater. Sci. Eng., 22, 035001, 2014.

Wang, L., Mi, J., and Guo, Z.: A modified lattice Bhatnagar–Gross–Krook model for convection heat transfer in porous media, Int. J. Heat Mass Transfer., 94, 269-291, 2016.

Wang, S., Elsworth, D., and Liu, J.: A mechanistic model for permeability evolution in fractured sorbing media, J. Geophys. Res, 117, B06205, doi:10.1029/2011JB008855, 2012.

Wu, M., Wu, J.F., and Wu, J.C.: Simulation of DNAPL migration in heterogeneous translucent porous media based on estimation of representative elementary volume, J. Hydrol., 553, 276-288, 2017.

Wu, M., Wu, J.F., Wu, J.C., and Hu, B.X.: Effects of microarrangement of solid particles on PCE migration and its remediation in porous media, Hydrol. Earth Syst. Sci., 22, 1001-1015, 2018.

Table 1. Experimental conditions

Experiment	I	II	III
Sandbox dimensions (cm)	20×15	60×45	60×45
~~Packed translucent silica sand~~Background translucent silica sand	F40/50	F20/30	F20/30
Medium condition	Homogeneity	Homogeneity	Heterogeneity
Median grain diameter (mm)	0.36	0.72	0.72
Permeability (m^2)	4.25×10^{-11}	1.35×10^{-10}	1.35×10^{-10}
V_{PCE} (ml)	9	32	40
Injection rate (ml/min)	0.5	0.5	0.5

Table 2. Criteria of REV estimation

Criterion	Equation
The coefficient of variation	$C_V^i = \frac{\hat{s}}{\overline{\varphi}_i}$
entropy dimension	$DI^i \approx \frac{\sum_{j=1}^{m(i)} \mu_j(L_\varepsilon)\log \mu_j(L_\varepsilon)}{\log L_\varepsilon}$
the relative gradient error	$\varepsilon_g^i = \left\lvert \frac{\varphi^{i+1} - \varphi^{i-1}}{\varphi^{i+1} + \varphi^{i-1}} \right\rvert \frac{1}{\Delta L}$
New criterion	$\chi^i = \frac{\lvert \delta_{i+1} - \delta_{i-1} \rvert}{\delta_i \Delta L}$

Table 2~~3~~. The fitted equations of frequency for REVs of porosity, density and tortuosity

~~Experiment~~	~~I~~	~~II~~
~~θ-REV~~	$F=-2.01\times10^{-12}+\frac{1}{\sqrt{2\pi}\times1.50}e^{-\frac{(REV-4.35)^2}{2*1.50^2}}$ ~~(R^2=0.955)~~	$F=-5.30\times10^{-3}+\frac{1}{\sqrt{2\pi}\times3.35}e^{-\frac{(REV-8.05)^2}{2*3.35^2}}$ ~~(R^2=0.932)~~
~~ρ-REV~~	$F=-7.51\times10^{-26}+\frac{1}{\sqrt{2\pi}\times1.14}e^{-\frac{(REV-2.89)^2}{2*1.14^2}}$ ~~(R^2=0.969)~~	$F=-3.18\times10^{-12}+\frac{1}{\sqrt{2\pi}\times1.71}e^{-\frac{(REV-2.97)^2}{2*1.71^2}}$ ~~(R^2=0.989)~~
~~τ-REV~~	$F=-2.76\times10^{-15}+\frac{1}{\sqrt{2\pi}\times1.42}e^{-\frac{(REV-3.65)^2}{2*1.42^2}}$ ~~(R^2=0.774)~~	$F=-8.55\times10^{-8}+\frac{1}{\sqrt{2\pi}\times2.15}e^{-\frac{(REV-4.30)^2}{2*2.15^2}}$ ~~(R^2=0.850)~~

~~*F represents the frequency of REV, θ represents porosity, ρ represents density, τ represents tortuosity~~

Experiment		I	II	III
θ-REV	ω	-2.11×10^{-4}	-1.45×10^{-3}	7.63×10^{-4}
	~~ε~~ϵ	1.73	3.45	3.18
	ν	4.35	7.90	6.50
	R^2	0.938	0.924	0.907
ρ-REV	ω	-6.51×10^{-4}	-2.51×10^{-4}	1.51×10^{-3}
	~~ε~~ϵ	1.08	1.66	2.40
	ν	2.89	2.97	3.70
	R^2	0.967	0.990	0.859
τ-REV	ω	-3.36×10^{-4}	-2.04×10^{-4}	1.29×10^{-3}
	~~ε~~ϵ	1.39	2.15	1.20
	ν	3.65	4.20	1.05
	R^2	0.769	0.875	0.919

*θ represents porosity, ρ represents density, τ represents tortuosity; ω, ϵ and ν are fitted parameters of the model

Table 34. The fitted equations between average value of REV and d_I, d_m

Experiment	I		II	
	S_o-REV	A_{OW}-REV	S_o-REV	A_{OW}-REV
d_m	$\overline{REV} = -1.67\times10^{-3}d_m^2 + 0.193d_m + 2.72$ (R^2=0.807)	$\overline{REV} = -6.10\times10^{-4}d_m^2 + 5.82\times10^{-2}d_m + 7.20$ (R^2=0.401)	$\overline{REV} = -4.08\times10^{-5}d_m^2 + 1.50\times10^{-2}d_m + 7.54$ (R^2=0.655)	$\overline{REV} = -1.92\times10^{-5}d_m^2 + 4.47\times10^{-3}d_m + 9.46$ (R^2=0.616)
d_I	$\overline{REV} = -1.97\times10^{-3}d_I^2 + 0.245d_I + 1.12$ (R^2=0.832)	$\overline{REV} = -1.47\times10^{-3}d_I^2 + 0.205d_I + 1.84$ (R^2=0.733)	$\overline{REV} = -3.94\times10^{-5}d_I^2 + 7.80\times10^{-3}d_I + 8.50$ (R^2=0.327)	$\overline{REV} = -1.92\times10^{-5}d_m^2 + 4.47\times10^{-3}d_m + 9.46$ (R^2=0.616)

Experiment		d_m	d_I
I	S_o-REV	$\overline{REV} = -1.67\times10^{-3}d_m^2 + 0.193d_m + 2.72$ (R^2=0.807)	$\overline{REV} = -1.97\times10^{-3}d_I^2 + 0.245d_I + 1.12$ (R^2=0.832)
	A_{OW}-REV	$\overline{REV} = -6.10\times10^{-4}d_m^2 + 5.82\times10^{-2}d_m + 7.20$ (R^2=0.401)	$\overline{REV} = -1.47\times10^{-3}d_I^2 + 0.205d_I + 1.84$ (R^2=0.733)
II	S_o-REV	$\overline{REV} = -4.08\times10^{-5}d_m^2 + 1.50\times10^{-2}d_m + 7.54$ (R^2=0.655)	$\overline{REV} = -3.94\times10^{-5}d_I^2 + 7.80\times10^{-3}d_I + 8.50$ (R^2=0.327)
	A_{OW}-REV	$\overline{REV} = -1.92\times10^{-5}d_m^2 + 4.47\times10^{-3}d_m + 9.46$ (R^2=0.616)	$\overline{REV} = -1.92\times10^{-5}d_I^2 + 4.47\times10^{-3}d_I + 9.46$ (R^2=0.616)
III	S_o-REV	$\overline{REV} = -6.06\times10^{-6}d_m^2 + 2.27\times10^{-3}d_m + 7.76$ (R^2=0.153)	$\overline{REV} = 1.69\times10^{-5}d_I^2 - 1.21\times10^{-2}d_I + 9.62$ (R^2=0.236)
	A_{OW}-REV	$\overline{REV} = -8.71\times10^{-6}d_m^2 + 5.66\times10^{-3}d_m + 11.5$ (R^2=0.115)	$\overline{REV} = -1.50\times10^{-5}d_I^2 + 7.88\times10^{-3}d_I + 11.4$ (R^2=0.150)

*$\overline{REV}$ $\overline{REV}$ is the average value of REV size, d_m is the distance from mass center of PCE plume to the cell contained in PCE plume, d_I is the distance from injection point to the cell contained in PCE plume

Table 45. The fitted relationship between REV and S_o

Experiment	I	II
S_o-REV	$REV = -2.13 \times \ln S_o + 0.876$ (R^2=0.466)	$REV = -0.961 \times \ln S_o + 1.09$ (R^2=0.415)
A_{OW}-REV	$REV = 2.27e^{2.70 * S_o}$ (R^2=0.366)	$REV = 1.70e^{3.30 * S_o}$ (R^2=0.500)

Experiment	S_o-REV	A_{OW}-REV
I	$REV = -2.13 \times \ln S_o + 0.876$ (R^2=0.466)	$REV = 2.27e^{2.70 \times S_o}$ (R^2=0.366)
II	$REV = -0.961 \times \ln S_o + 1.09$ (R^2=0.415)	$REV = 1.70e^{3.30 \times S_o}$ (R^2=0.500)
III	$REV = -1.40 \times \ln S_o + 3.96$ (R^2=0.538)	$REV = 2.05e^{3.22 \times S_o}$ (R^2=0.573)

Figure Captions

Figure 1. ~~(a) System Device for acquisition of properties of translucent material; (b) The infinitesimal selected from translucent porous media packed in 2D sandbox;~~ (a~~c~~) Variable changes as measured scale (L) increment in conceptual curve (Costanza-Robinson et al., 2011); (b~~d~~) Scale effect and the cuboid image window geometry; (c) System Device for acquisition of parameters (porosity and density, etc.) of translucent material; (d) The infinitesimal selected from translucent porous media packed in 2D sandbox.

Figure 2. (a) The system sandbox equipment of Experiment-I; (b) The system sandbox equipment of Experiment-II; (c) The system sandbox equipment of Experiment-III

Figure 3. (a) The emergent light intensity, porosity, permeability and tortuosity of 2D translucent silica sand for Experiments-I-III~~ and II~~; (b) The PCE saturation of Experiments-I-III~~ and II~~ during 0~1523 min and observation cells

Figure 4. (a) The change of porosity (θ), associated coefficient of variation (C_V^i ~~C_V^i~~), entropy dimension (DI^i ~~DI^i~~), the relative gradient error (ε_g^i ~~ε_g^i~~), and new criterion-χ^i for observation cells as cuboid window scale (L) increases; (b) The change of PCE saturation (S_o), associated C_V^i ~~C_V^i~~, DI^i ~~DI^i~~, ε_g^i ~~ε_g^i~~, and χ^i for observation cells as cuboid window scale (L) increases

Figure 5. (a) The distributions of minimum REV sizes of porosity, sand density and tortuosity for Experiments-I-III~~ and II~~; (b) The frequency of minimum REV sizes of Experiments and fitted models

Figure 6. (a) The distributions of S_o-REV sizes during 0~1523 min for Experiments-I-III

and II; (b) The distributions of A_{OW}-REV sizes during 0~1523 min for Experiments-I-III and II

Figure 7. (a) The mass center coordinate of PCE plume, GTP, plume area and the mean, standard deviation of S_o-REV and A_{OW}-REV during 0~1523 minThe mass center coordinate of PCE plume and the change of average REV size as the distance d_I, d_m increases; (b) The mean, standard deviation of S_o-REV and A_{OW}-REV during 0~1523 min The change of average REV size as the distance d_I, d_m increases and fitted relationship between REV sizes and S_o for Experiments-I and II

Fig. 1

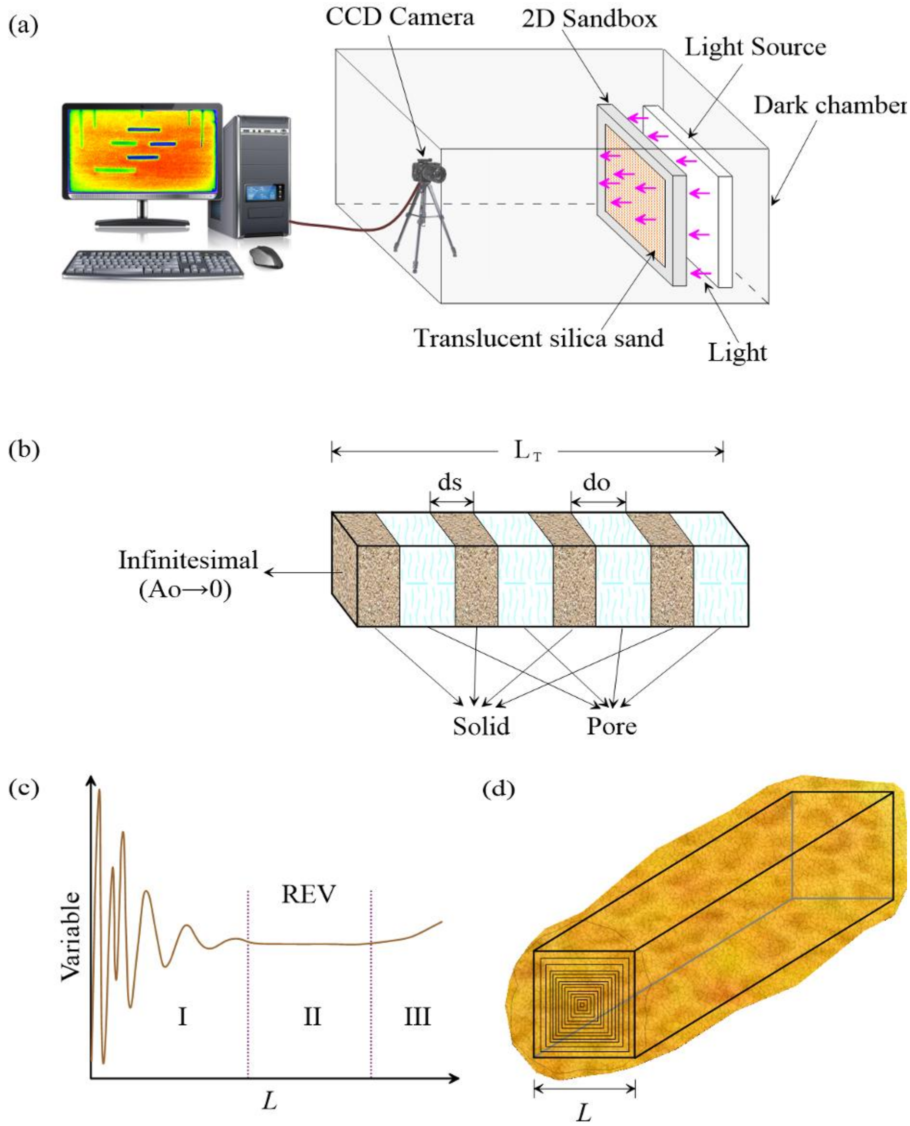
(a)
CCD Camera
2D Sandbox
Light Source
Dark chamber
Translucent silica sand
Light
(b)
L T
ds
do
Infinitesimal
(Ao→0)
Solid
Pore
(c)
Variable
REV
I
II
III
L
(d)
L

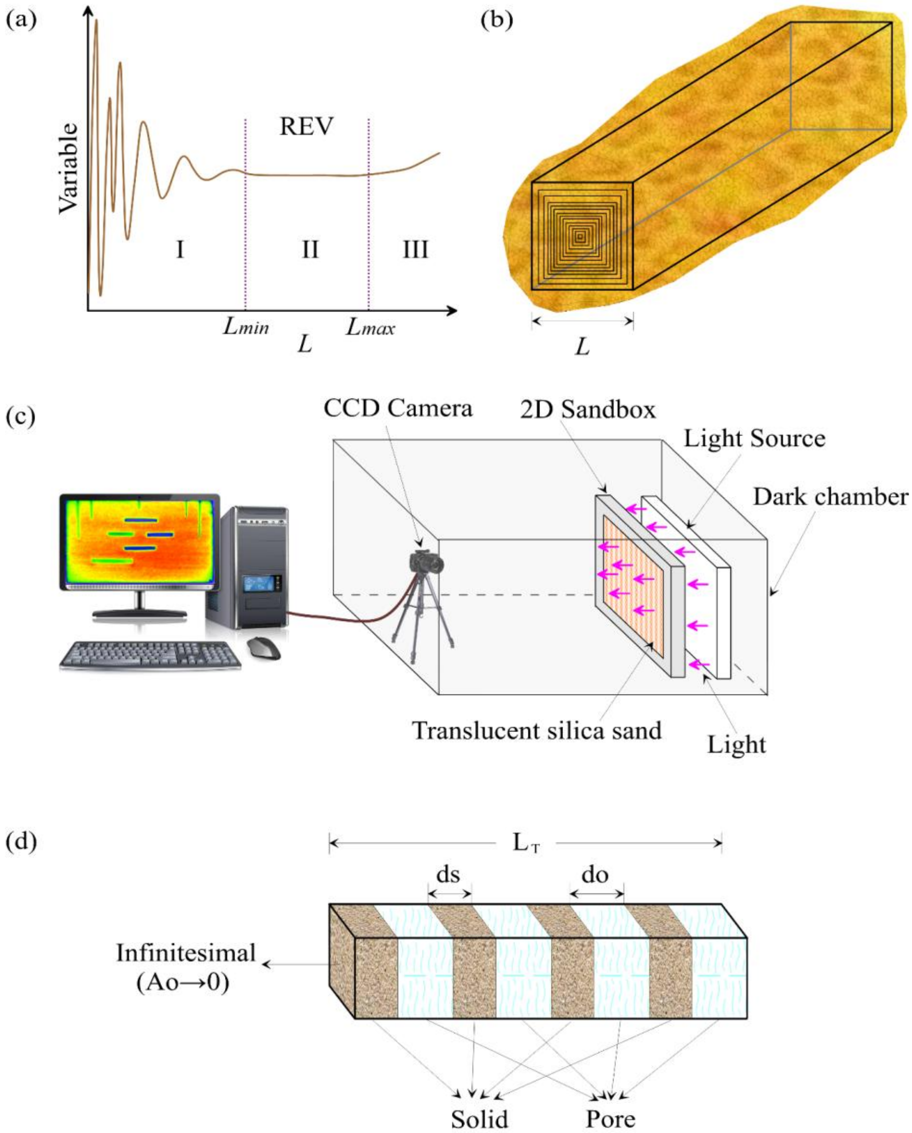
(a)
Variable
REV
I
II
III
Lmin
Lmax
L
(b)
L
(c)
CCD Camera
2D Sandbox
Light Source
Dark chamber
Translucent silica sand
Light
(d)
LT
ds
do
Infinitesimal
(Ao→0)
Solid
Pore

Fig. 2

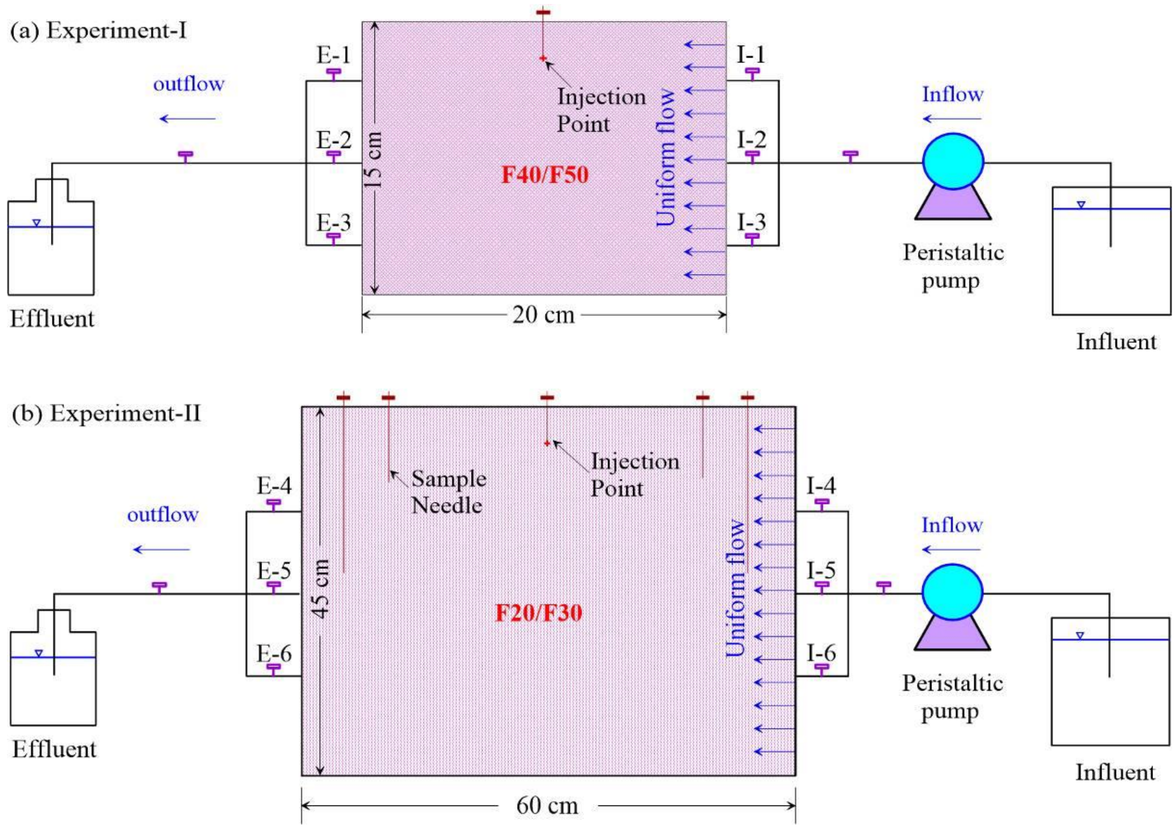

(a) Experiment-I
outflow
E-1
E-2
E-3
15 cm
Injection Point
F40/F50
Uniform flow
I-1
I-2
I-3
Inflow
Peristaltic pump
Effluent
20 cm
Influent
(b) Experiment-II
Sample Needle
Injection Point
E-4
E-5
E-6
outflow
45 cm
F20/F30
Uniform flow
I-4
I-5
I-6
Inflow
Peristaltic pump
Effluent
Influent
60 cm

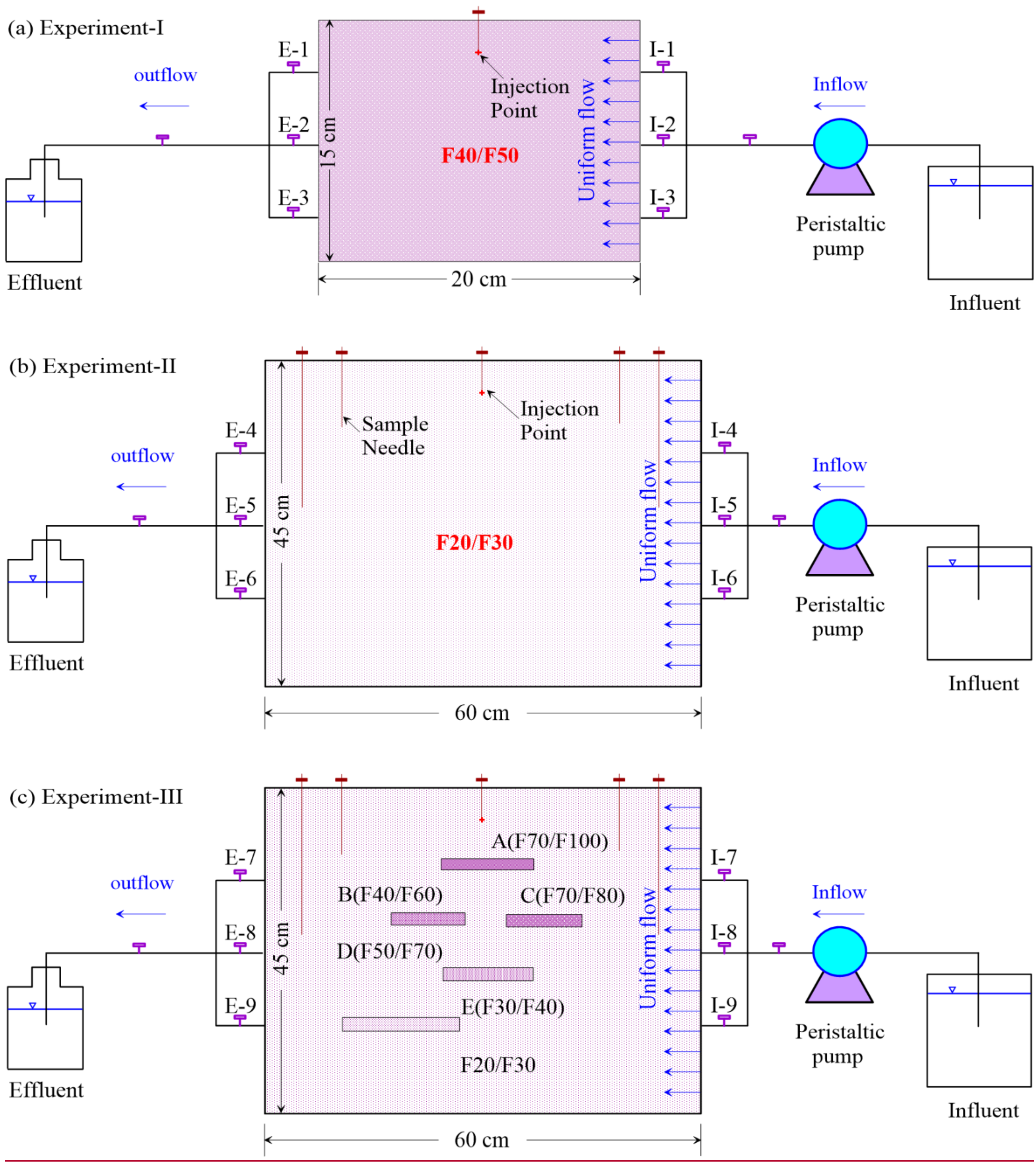
(a) Experiment-I
E-1
E-2
E-3
outflow
Injection
Point
15 cm
F40/F50
Uniform flow
I-1
I-2
I-3
Inflow
Peristaltic
pump
Effluent
20 cm
Influent
(b) Experiment-II
E-4
E-5
E-6
outflow
Sample
Needle
Injection
Point
45 cm
F20/F30
Uniform flow
I-4
I-5
I-6
Inflow
Peristaltic
pump
Effluent
60 cm
Influent
(c) Experiment-III
E-7
E-8
E-9
outflow
A(F70/F100)
B(F40/F60)
C(F70/F80)
D(F50/F70)
E(F30/F40)
F20/F30
45 cm
Uniform flow
I-7
I-8
I-9
Inflow
Peristaltic
pump
Effluent
60 cm
Influent

Fig. 3

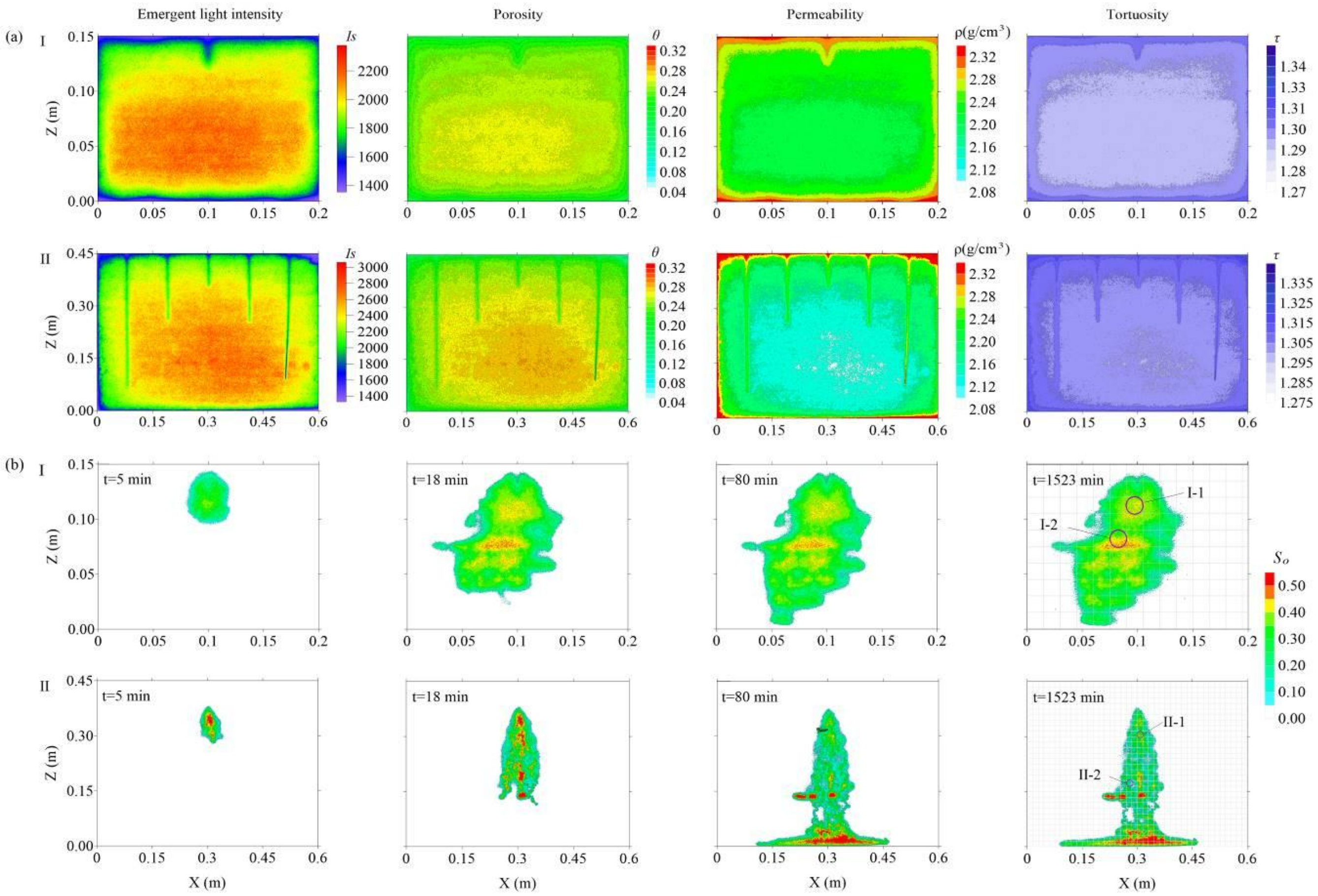

(a)
Emergent light intensity
Porosity
Permeability
Tortuosity
I
II
Is
θ
ρ(g/cm³)
τ
Z (m)
(b)
t=5 min
t=18 min
t=80 min
t=1523 min
I-1
I-2
II-1
II-2
S_o
X (m)

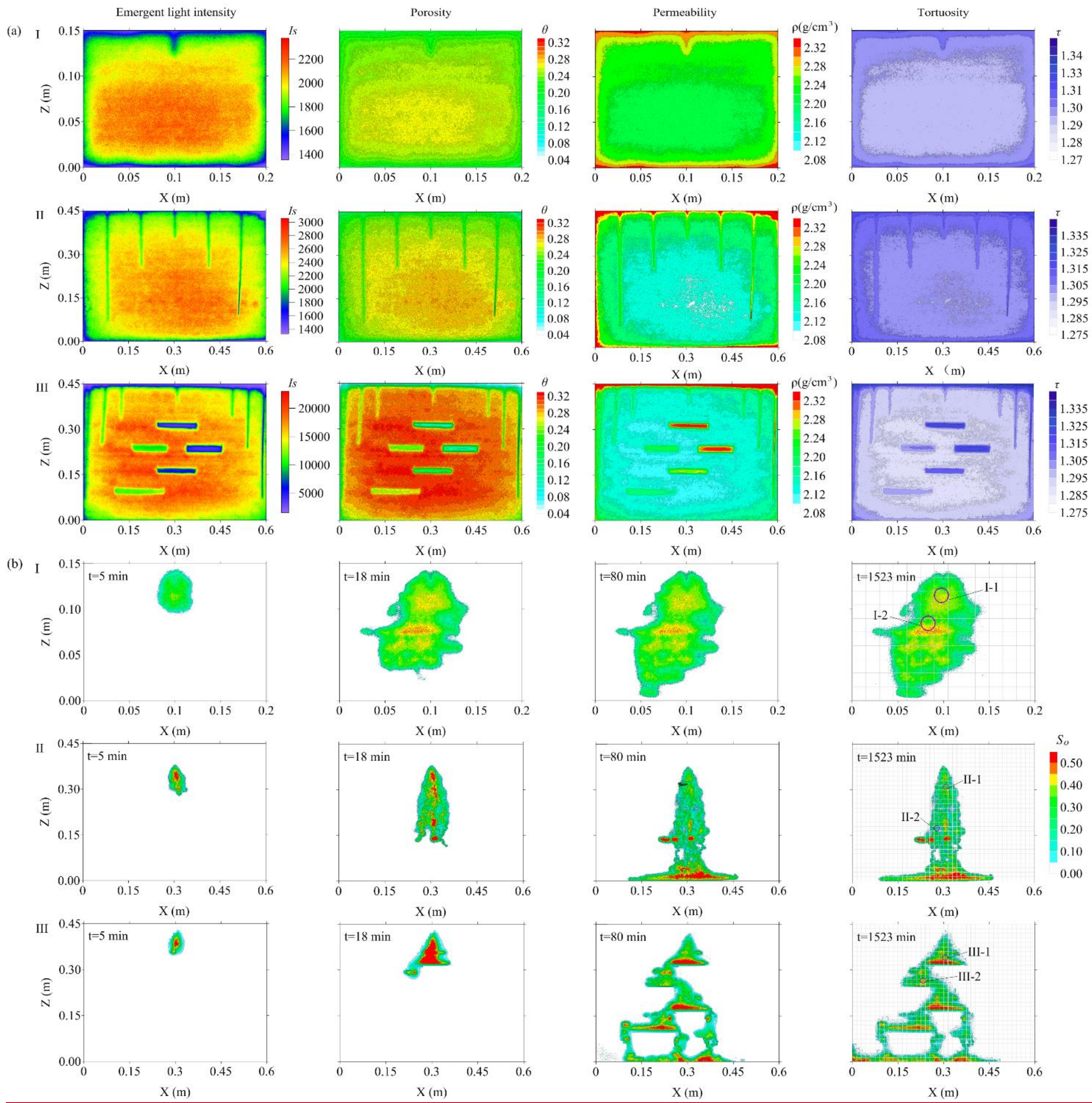

(a)
Emergent light intensity
Porosity
Permeability
Tortuosity
I
II
III
Is
θ
ρ(g/cm³)
τ
Z (m)
X (m)
(b)
t=5 min
t=18 min
t=80 min
t=1523 min
I-1
I-2
II-1
II-2
III-1
III-2
So

Fig. 4

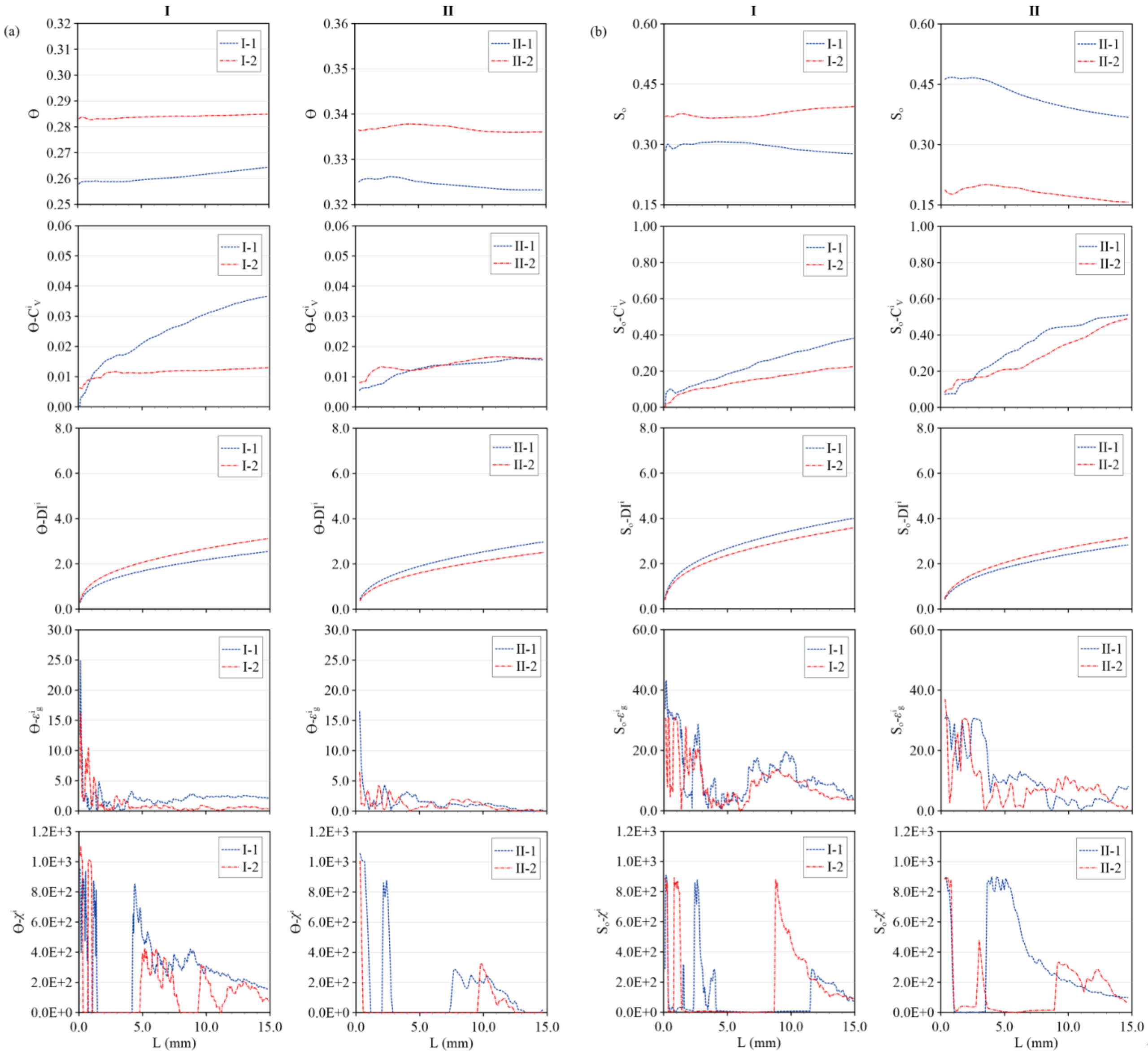
(a)
(b)
I
II
I-1
I-2
II-1
II-2
Θ
Θ-C^i_V
Θ-DI^i
Θ-ε^i_g
Θ-χ^i
S_o
S_o-C^i_V
S_o-DI^i
S_o-ε^i_g
S_o-χ^i
L (mm)

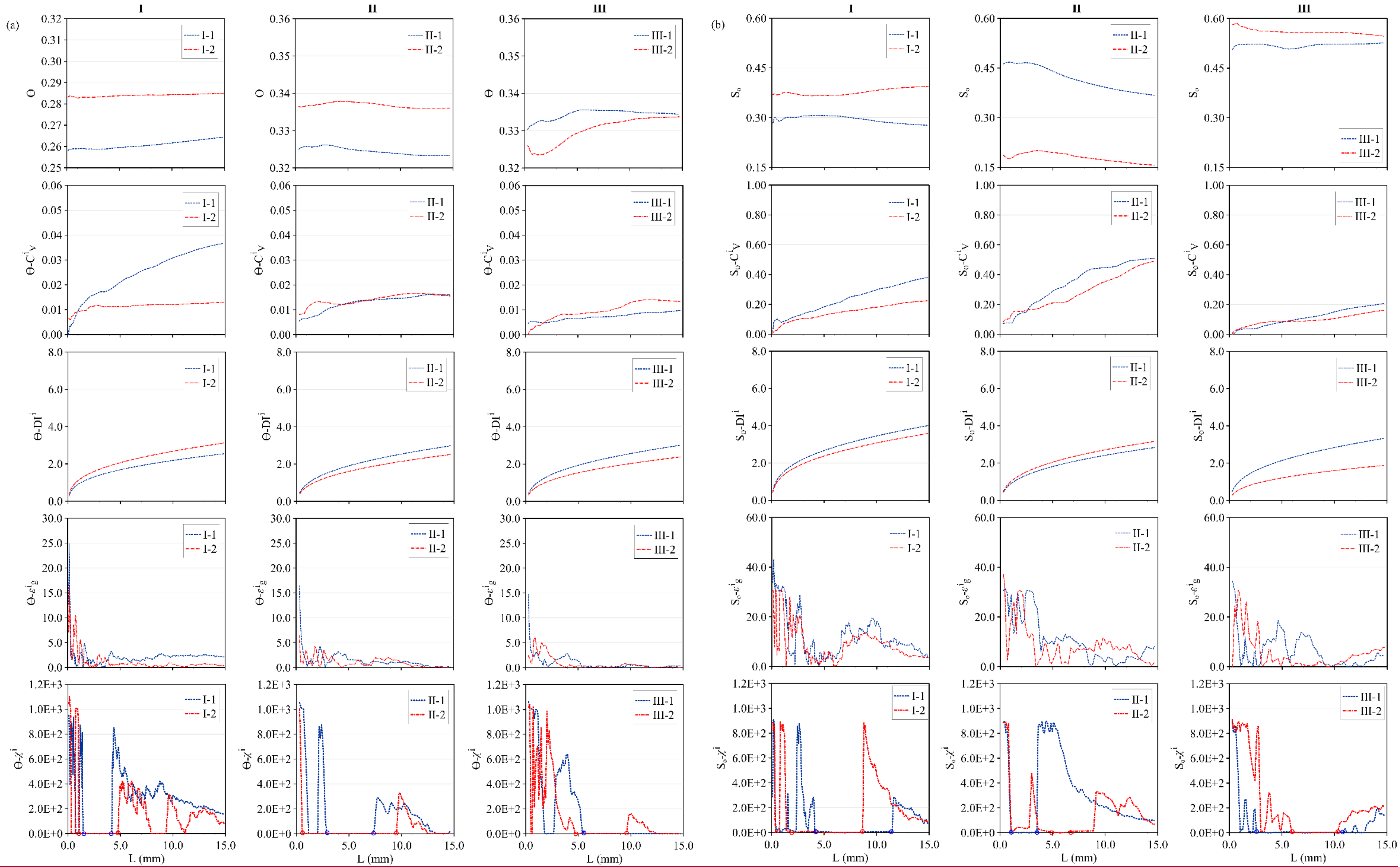
(a)
(b)
I
II
III
Θ
S₀
Θ-C^i_V
S₀-C^i_V
Θ-DI^i
S₀-DI^i
Θ-ε^i_g
S₀-ε^i_g
Θ-χ^i
S₀-χ^i
I-1
I-2
II-1
II-2
III-1
III-2
L (mm)

702 **Fig. 5**

703

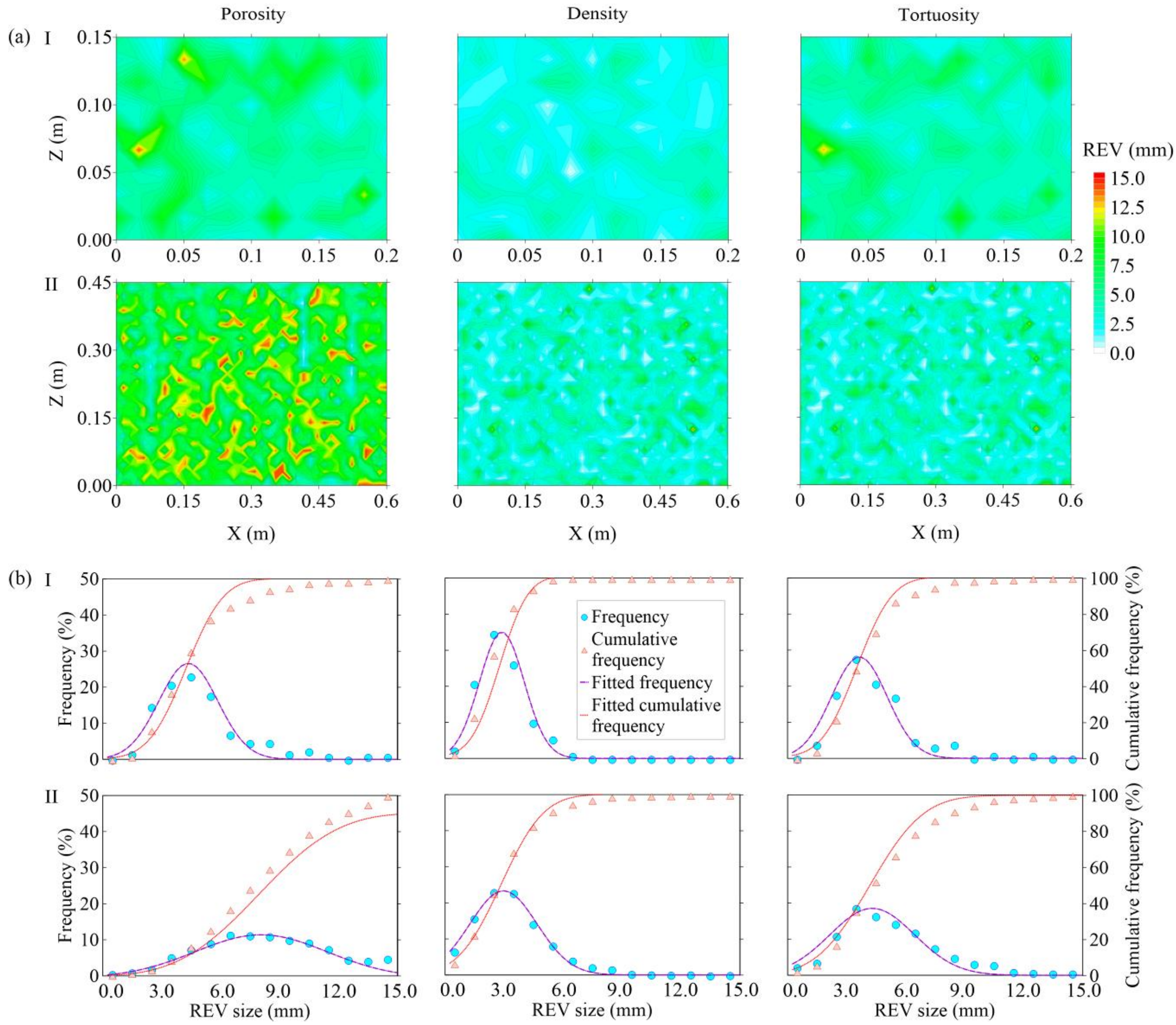

704

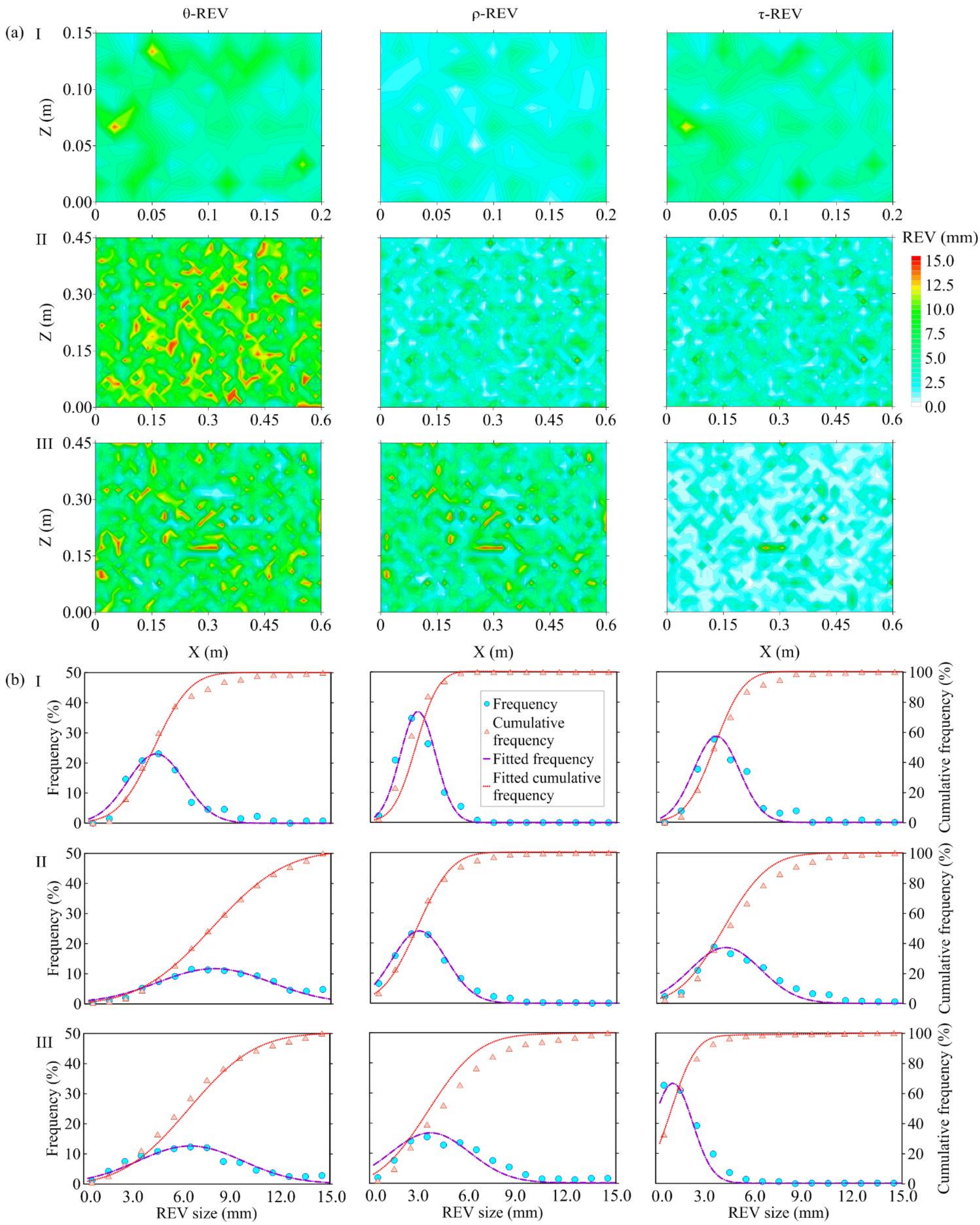

θ-REV
ρ-REV
τ-REV
(a)
I
II
III
Z (m)
X (m)
REV (mm)
15.0
12.5
10.0
7.5
5.0
2.5
0.0
(b)
Frequency (%)
Cumulative frequency (%)
Frequency
Cumulative frequency
Fitted frequency
Fitted cumulative frequency
REV size (mm)

Fig. 6

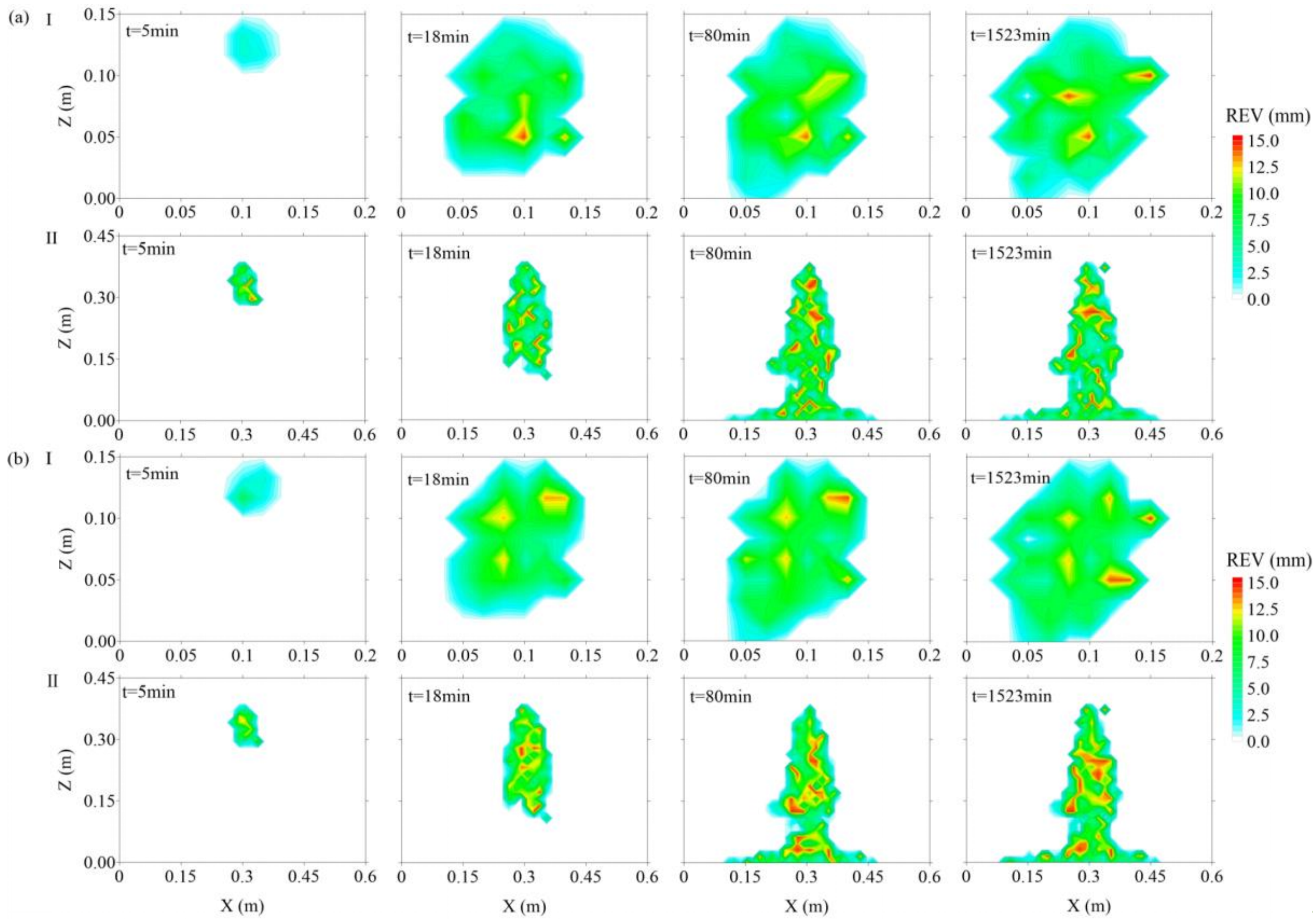
(a)
I
II
(b)
I
II
t=5min
t=18min
t=80min
t=1523min
Z (m)
X (m)
REV (mm)
15.0
12.5
10.0
7.5
5.0
2.5
0.0
0
0.05
0.1
0.15
0.2
0.00
0.05
0.10
0.15
0.30
0.45
0.3
0.6

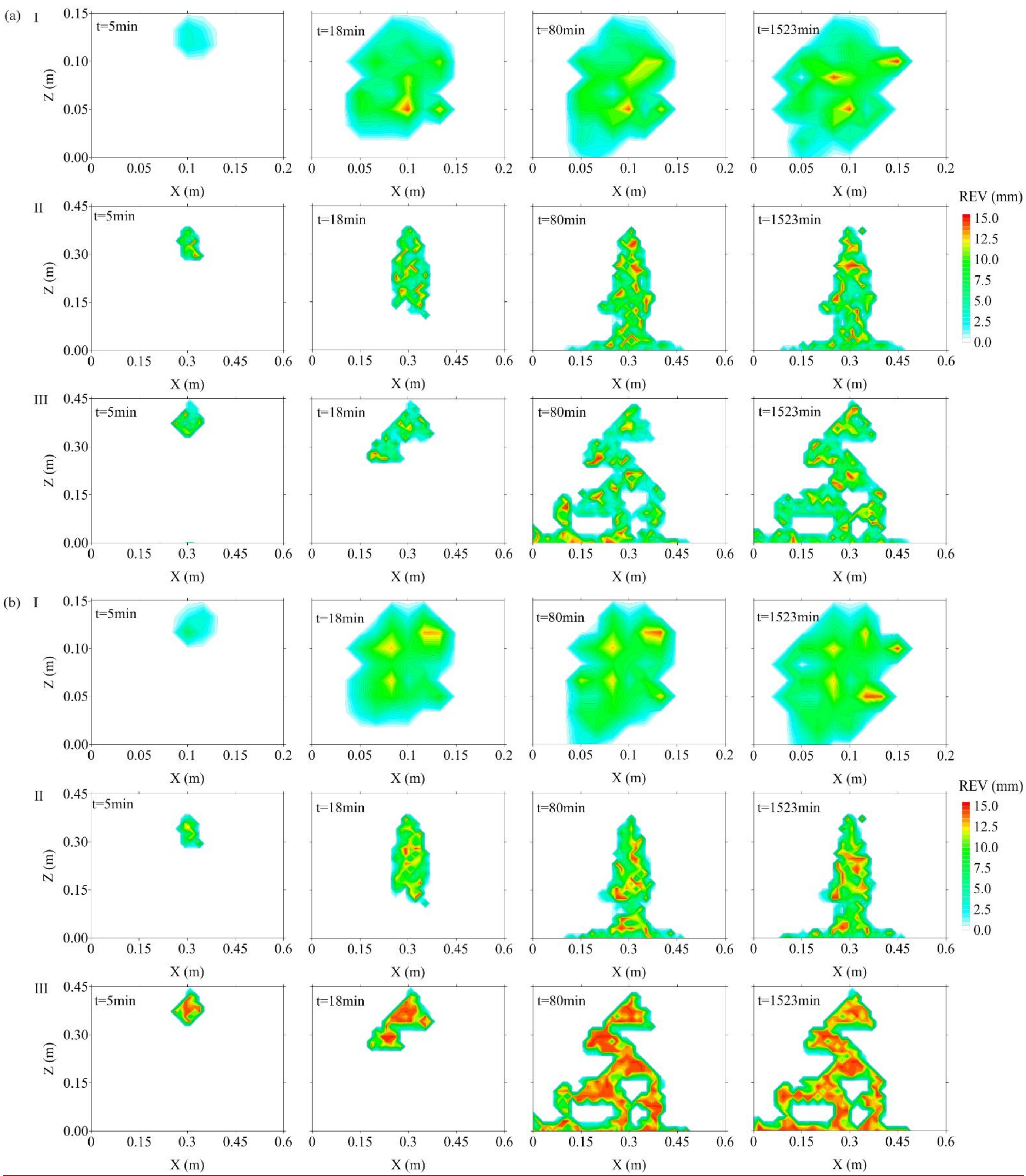

(a)
I
II
III
(b)
t=5min
t=18min
t=80min
t=1523min
Z (m)
X (m)
REV (mm)
15.0
12.5
10.0
7.5
5.0
2.5
0.0

Fig. 7

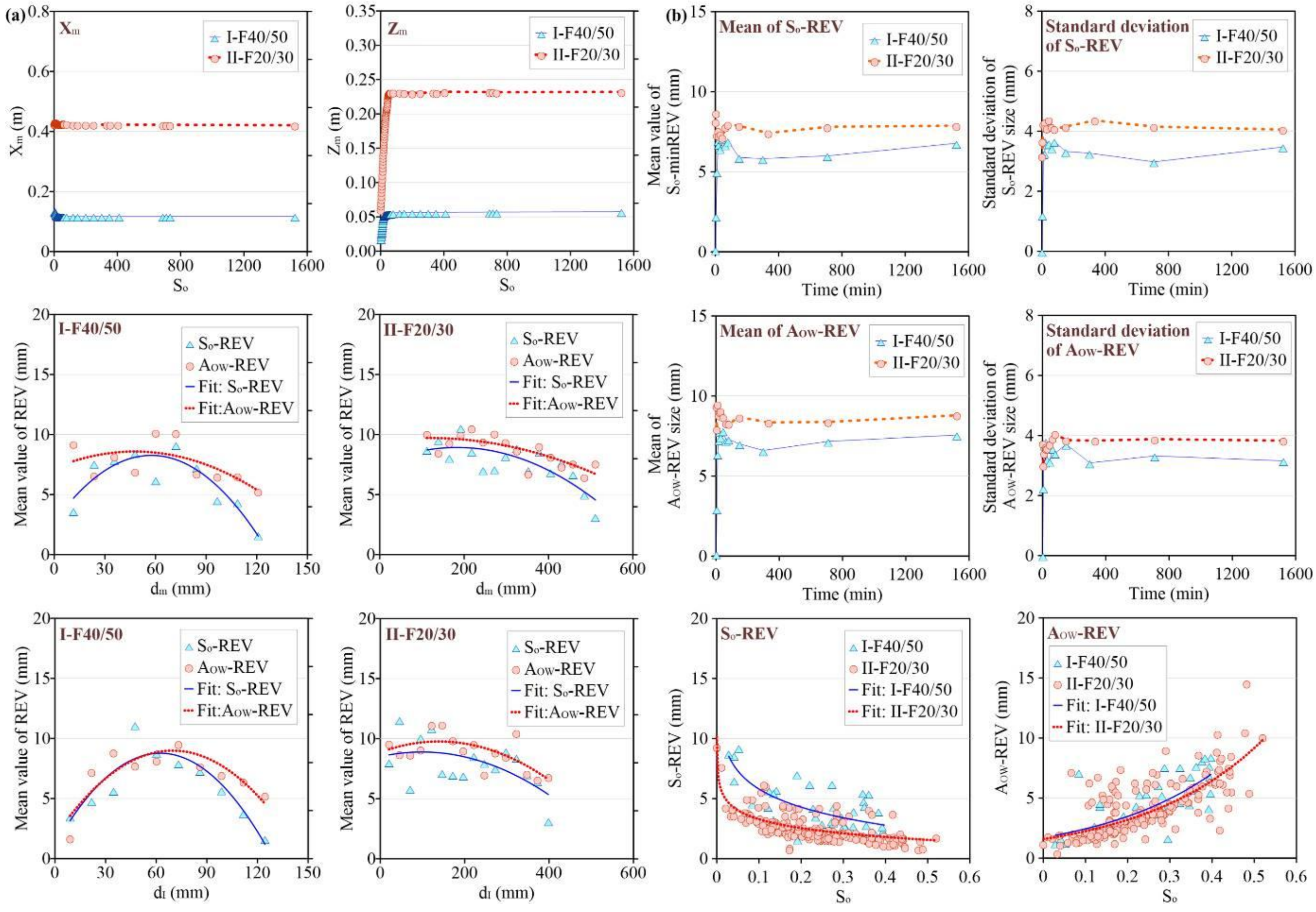
(a)
Xm
I-F40/50
II-F20/30
Xm (m)
So
Zm
Zm (m)
(b)
Mean of So-REV
Mean value of So-minREV (mm)
Time (min)
Standard deviation of So-REV
Standard deviation of So-REV size (mm)
I-F40/50
II-F20/30
So-REV
Aow-REV
Fit: So-REV
Fit:Aow-REV
Mean value of REV (mm)
dm (mm)
Mean of Aow-REV
Mean of Aow-REV size (mm)
Standard deviation of Aow-REV
Standard deviation of Aow-REV size (mm)
dl (mm)
So-REV
So-REV (mm)
Fit: I-F40/50
Fit: II-F20/30
Aow-REV
Aow-REV (mm)

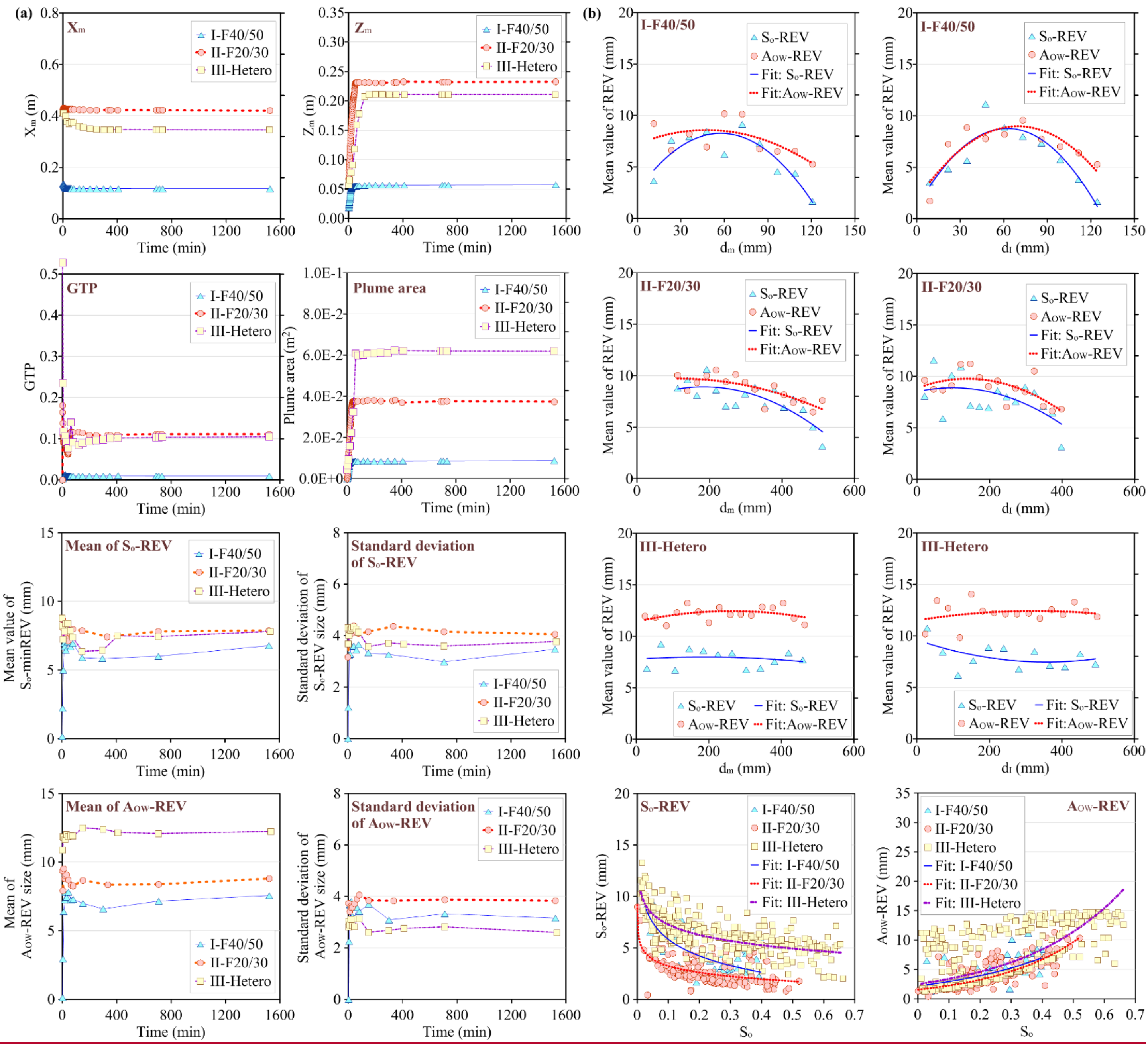

(a)
Xm
I-F40/50
II-F20/30
III-Hetero
Xm (m)
Time (min)
Zm
Zm (m)
GTP
Plume area
Plume area (m2)
Mean of So-REV
Mean value of So-minREV (mm)
Standard deviation of So-REV
Standard deviation of So-REV size (mm)
Mean of Aow-REV
Mean of Aow-REV size (mm)
Standard deviation of Aow-REV
Standard deviation of Aow-REV size (mm)
(b)
I-F40/50
II-F20/30
III-Hetero
So-REV
Aow-REV
Fit: So-REV
Fit:Aow-REV
Mean value of REV (mm)
dm (mm)
dl (mm)
So-REV (mm)
Aow-REV (mm)
Fit: I-F40/50
Fit: II-F20/30
Fit: III-Hetero
So